Stability of Gravel Bars & Bedload Transport in Paint Branch Creek

Andrew J. Kosiba

April 28, 2008

Advisors:
Dr. Karen Prestegaard
Zach Blanchet

University of Maryland: Department of Geology

Abstract: Streams in urbanized watersheds respond to changes in water and sediment supply; these channel changes create many problems for local communities. The increase in impervious surfaces in urban settings can cause an increase in overbank flooding and/or the erosion of stream banks. Where buildings are at risk, these problems are often addressed by channel restoration projects, particularly bank stabilization. In my research I examined an unconstrained reach of river where gravel bars are forming. The study site is a gravel-bar complex within the PBS channel downstream of Cherry Hill road. In the areas where the gravel bars are being formed, the channel widths are 2-3 times wider than adjacent reaches. There is concern that if the channel widening is not mitigated by erosion control measures, that the channel will continue to erode. In my research, I tested the hypothesis that gravel bar formation actually results in channel stabilization by increasing channel width, decreasing channel depth, and therefore shear stress within the braided reach. My research was based on determining 3 variables needed to analysis the dimensionless shear stress, depth, grain size and energy gradient. I found that the channel initially widens at the bar head, and becomes less wide downstream. The upstream portion of the divided reach has lower average shear stresses than the upstream reach, but the bar tail is a zone of active bed and bank scour and sediment transport. Shear stresses over the bar top are significantly lower than in the channels.

Introduction and Previous Work

Paint Branch stream (PBS) is the main stream in the portion of the Anacostia watershed that includes College Park Maryland. The analysis of the Paint Branch gravel bars and bedload transport have significant importance to the College Park community. Currently there are large gravel bars present in the channel of the PBS, particularly on campus and downstream, of The University of Maryland. One of these gravel bars was just removed in a costly stream stabilization project. The large gravel bars in certain regions of the PBS cause concern because the gravel bars decrease the volume of the channel, reducing the capacity of the channel to transport flood discharges. They can also divert flow and enhance bank erosion. My research focused on one section of the Paint Branch Stream in which gravel bars are present in the College Park area. The location of research will be along Little Paint Branch Creek downstream of Cherry Hill Road.

The PBS is an armored, gravel-bed stream. The surface grains protect the subsurface grains from transport until a critical shear stress is achieved to move the larger grains. The surface grains act like obstacles that must be moved out of the way for the subsurface grains and total bedload transport downstream (Wiberg and Smith, 1989; Milhous, 1973 in Buffington, 1997). Bankfull stage is the largest discharge that the channel can contain without overbank flooding. In channels with wide floodplains, shear stresses increase up to the bankfull stage and the flow above bankfull stage is carried primarily by the floodplain, without a significant increase in channel shear stresses.

The main point of my research was to determine whether or not PBS has stable gravel bars at bankfull stage. There have been decades of prior research on a streams ability to move the sediment of gravel-bedded streams. (Barry, 2004; Buffington et.al., 1997; Constantine et.al., 2003; Dietrich, 1898; Goodwin, 2004; Hjulstrom, 1939; Miller, 1997; Parker, 1978; Renger, 2007; Shields, 1936; Wilson, 2005) I applied prior research to determine whether or not PBS has

the ability at bankfull stage to move the gravel bed sediment of the stream out of the College Park region. Channel restoration has occurred along the PBS in the College Park region.

The area I researched an area that has not undergone restoration but has many gravel bars present in the middle of the stream's channel. In gravel bed streams, bedload transport is initiated when the flow depth and gradient are sufficient to move the particles from the bed. This threshold can be expressed as a critical shear stress. By taking the ratio of the fluid shear stress to the grain resisting forces, we can also evaluate a critical dimensionless shear stress for the initiation of motion.

There are a series of equations that are needed to be applied to determine the presence of stable or mobile gravel bars in the PBS system. The first equation of the series is used to calculate the boundary shear stress of the stream. The shear stress (T) is a force per area measurement that represents the downslope component force of water acting on the channel boundary.

$\tau = \rho g R S$

g= acceleration due to gravity 9.814 m/s^2
ρ = water density (1000 kg/m^3)
R = Hydraulic radius (A/P) often similar to depth (m) for large widths
S = energy gradient (water surface gradient in straight reaches).

There are two variables that need to be measured in the field of the study reach. The first variable, R, can be determined through the survey of a cross-section. Channel survey data can also be used to determine the distribution of channel depths and thus the distribution of shear stress throughout the channel cross section. The second variable, S, can be determined through a survey of surface water elevation over a distance.

In my research, I evaluated whether the bankfull channel is capable of moving the sediment along its boundary. I will be conducting an initiation of motion study. This analysis of the sediment motion within a fluvial environment was first developed by Shields (1936) and Hjulstrom (1935). Figure 1 is a graphical representation of Hjulstrom's work, which relates Velocity to grain size, showing critical areas between Transportation, Deposition, and Erosion of sediment.

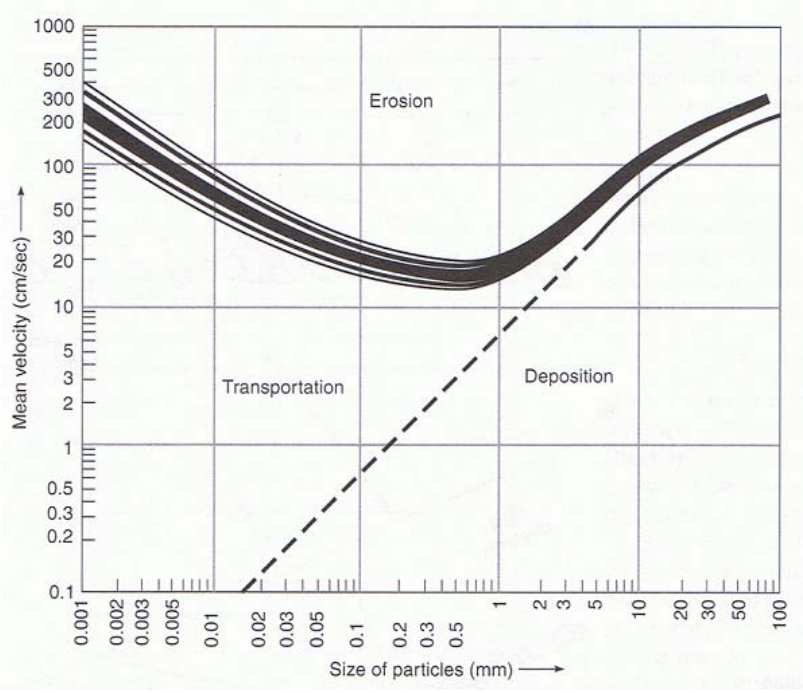

Figure 1: Graph representing Hjulstrom work relating mean fluid velocity vs. the size of the particles (Hjulstrom (1939) in Ritter et. al., 2002, p197)

Figure 1 indicates how the mean velocity affects particle erosion and deposition. Small particles, once they are eroded from the bed are kept in the flow by turbulence. Large particles, such as those in Paint Branch Creek, are not carried by suspension, but by moving in contact with the bed, which is called bedload transport. The onset of bedload transport is related to the bed shear stress. Shields ideas and work describe the onset of bedload transport by relating dimensionless shear stress to grain Reynolds number as seen in Figure 2.

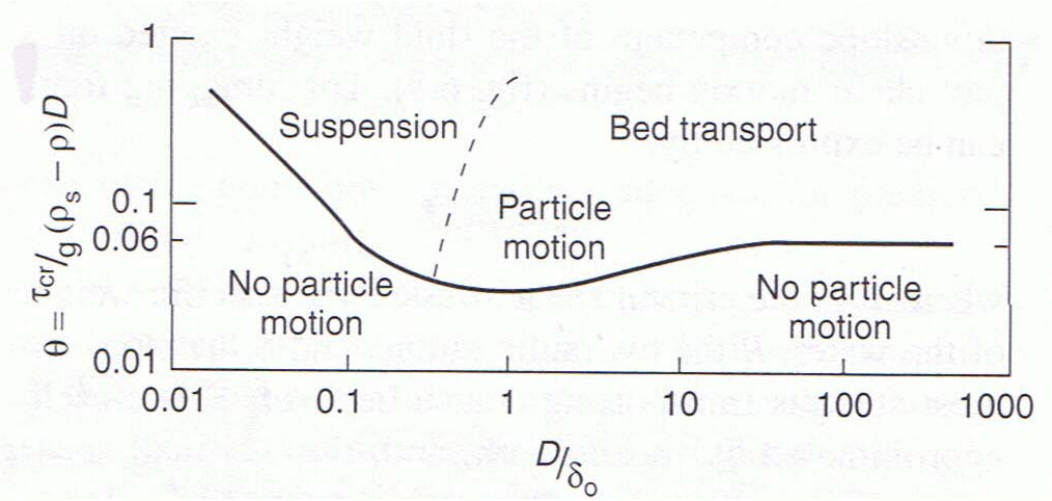

Figure 2: The Graph representing Shields work represents the Dimensionless shear stress to Reynolds number (D/δ_0). (Ritter et. al., 2002, p 198, "Shield curve for the entrainment of bed particles where D is grain diameter, $_{cr}$ is critical shear stress, ρ_s is sediment density, ρ is fluid density, and δ_0 is the thickness of laminar sublayer").

Shields defined a dimensionless shear stress, which is the ratio of the fluid shear stress to the particle resisting forces. Shown in Figure 2 on the Y axis, the dimensionless shear stress (θ) equation can be represented as:

$$\theta = \tau/(g(\rho_s-\rho)D)$$

$\tau = \rho gRS$
ρ_s = Density of sediment (Quartz = 2,600 kg/m^3)
ρ = Density of Water (1000 kg/m^3)
g = acceleration due to gravity 9.814 m/s^2
D = grain size of surface material (from field sampling)

Shields' work determined that critical dimensionless shear stress, θ, equaled 0.06 for his experiments with homogenous sediment. Researchers in the 1970's started to realize that his work did not apply to heterogeneous sediment. Shields' work did not take into account the effect of large grain sizes that project in the flow over smaller sediment particles. Also Shields work did not take into effect banks. Figure 3 represents a surface from Paint Branch Creek which shows the distribution of surface grain sizes. As you can see from Figure 3 the larger clast shield or armor the smaller subsurface grains from mobility. Researchers have conducted field and laboratory studies to evaluate the critical dimensionless shear stress for heterogeneous sediment on stream channels (Milhous, 1973; Wiberg and Smith, 1989). They found that in a mixture of sediment, coarse particles (often taken to be D84) regulate the mobility of the surface layer by stabilizing the smaller particles. Because the large particles can move more easily over the smaller particles, the critical dimensionless shear stress for heterongeous sediment mixtures is less than found by Shields (1936) for homogeneous sediment . The critical dimensionless shear stress value was determined to be 0.045 (Miller et. al, 1977; Gessler, 1997 in Buffington, 1997) for naturally-sorted river bed sediment.

Gary Parker (1978) examined the question of how a channel could be stable and yet still transport bedload sediment. He determined that stable (threshold) channels move sediment in the deep parts of the channel, while not moving sediment near the banks. He found that stable gravel-bed channels occur when the critical shear stress is exceeded by 20% in the channel center, but not exceeded on the channel banks. We can test this by examining the dimensionless shear stress across the channel.

Figure 3: Photograph of the study site. 4 Channel cross sections were surveyed upstream of the gravel bar and 4 cross sections were surveyed through the bar reach.

Figure 4: Photograph of the gravel bar sediment that armors the subsurface material for total bedload movement.

Research Objectives:

Major gravel bars are forming within the channel of Paint Branch stream. Figure 3 is a photograph of the gravel bar complex researched that is forming in the middle of the channel. Field observations indicate that channel width in the gravel bar regions of the stream were 2-3x larger than in the non-bar reaches. At the study site, the stream banks have not been constrained, so the channel can migrate freely. The gravel bars in some reaches of the stream have vegetation growing on the bar surfaces, possibly indicating bar stabilization. Figure 4 is a photograph of the gravel size particles that armor the subsurface grains from bedload transport. If the gravel bars are not stable, the channels may continue to widen or the channel widening may propagate downstream. These observations lead to my main hypothesis:

Stream reaches with bar complexes are stabilized by width expansion, which lowers both channel depth and boundary shear stress to stabilize sediment: a) on the gravel bars, and b) within the channel.

Figure 5: Photograph taken looking upstream from the gravel bar reach of the stream. The bridge the cross in the picture is Cherry Hill Rd. Notice the relatively straightness of the channel prior to the gravel bar reach.

Choice of field site

The study site chosen was a gravel bar complex located downstream of Cherry Hill Road (fig. 5). This site was chosen because it is the first of a series of central gravel bars, and represents the transition from a straight reach to a braided segment. The transition is important because we make some assumptions that the straight reach is stable due to the fact it is able to transport

sediment downstream without the presents of gravel bars forming in the middle of the channel. Once the stream starts to form gravel bars the overall with of the channel widens by 2-3 times larger (fig. 3).

Field Methods

To test my hypothesis I collected field data. The main goal of the data collection was to evaluate channel shear stresses and grain size distributions in the channel. Average Boundary shear stress is determined from rgRS, which requires channel cross section and gradient data.

*Cross Section Surveys and error analysis of cross section surveys***:**

I surveyed eight cross-sections throughout the gravel bar complex to determine whether the gravel bar was stable at bankfull stage. Cross section surveys were conducted 1) upstream of the gravel bar complex, 2) throughout the gravel bar complex and 3) at the end of the gravel bar complex. The standard procedure I used to measure the cross-section was to survey elevations for 15-25 points in the channel and add the measurements where the channel changed shape, such as along the bank. For a Paint Branch Creek section that is 20 m wide, this was an average measurement interval of 1 m. The time required to make these measurements is less than one hour, including set-up.

To test the accuracy of the cross sections evaluated from this procedure, I increased the number of measurements by an order of magnitude. We surveyed elevations every 5 cm and recorded 383 elevations for a 19.10 meter wide cross-section. This cross section took 3 hours, with an additional three hours for data entry. I picked a cross-section to measure that had essentially two channels on either side of the gravel bar, which is located in the middle of the two channels. The cross-section was the typical profile of the channel in which the gravel bar was present

I considered the detailed survey to represent the "true" channel cross section. Therefore, the difference between this cross section and the one measured using standard intervals was considered to be a cross section measurement error. Next, I graphed and calculated the area from the 383 data points (Figure 6: a) then I graphed and calculated the area for the same cross-section removing all data points except for elevations recorded every meter starting at 0 meter and ending at 19.1 meters (20 data points) (Figure 6: b). The difference in area varied by 1.77 % for the area calculated under bankfull condition. This measurement error of 1.77% was considerably smaller than the variability measured at two cross sections 35 m apart which were 8.36 m^2 and 6.79 m^2. Therefore, the natural variability, which I need to measure, is much greater than the measurement error.

The perimeter varied a great deal more by 7.65 %. The perimeter variance is greater because the measurement of perimeter was fractal, which means that the shorter intervals that I used to measure the perimeter; you measured smaller perturbations and increased the perimeter length. Although average boundary shear stress is calculated using hydraulic radius, Area/perimeter, I calculated shear stress at depths across the channel; therefore local depth replaced R in the shear stress equation.

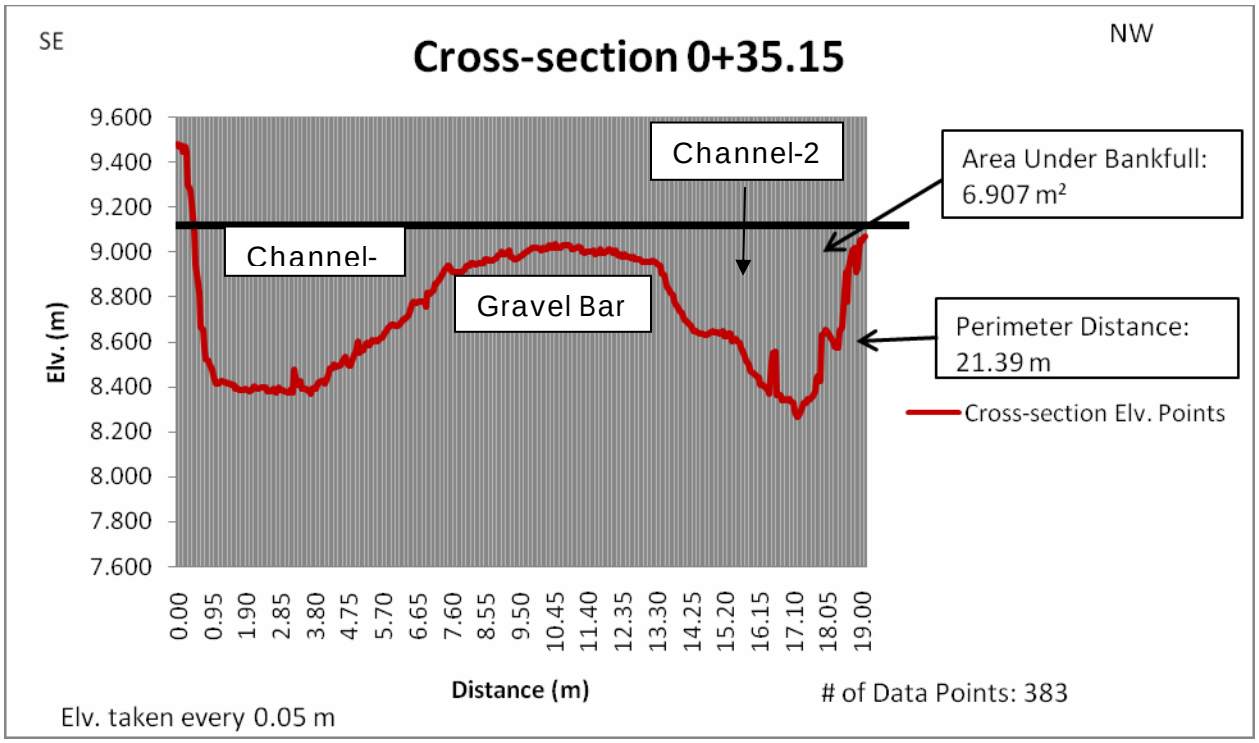

Figure 6: a) Graph of detailed data survey of a cross-section with measurements taken every 5 cm. Refer to Appendix A for data elevations recorded to create drafts.

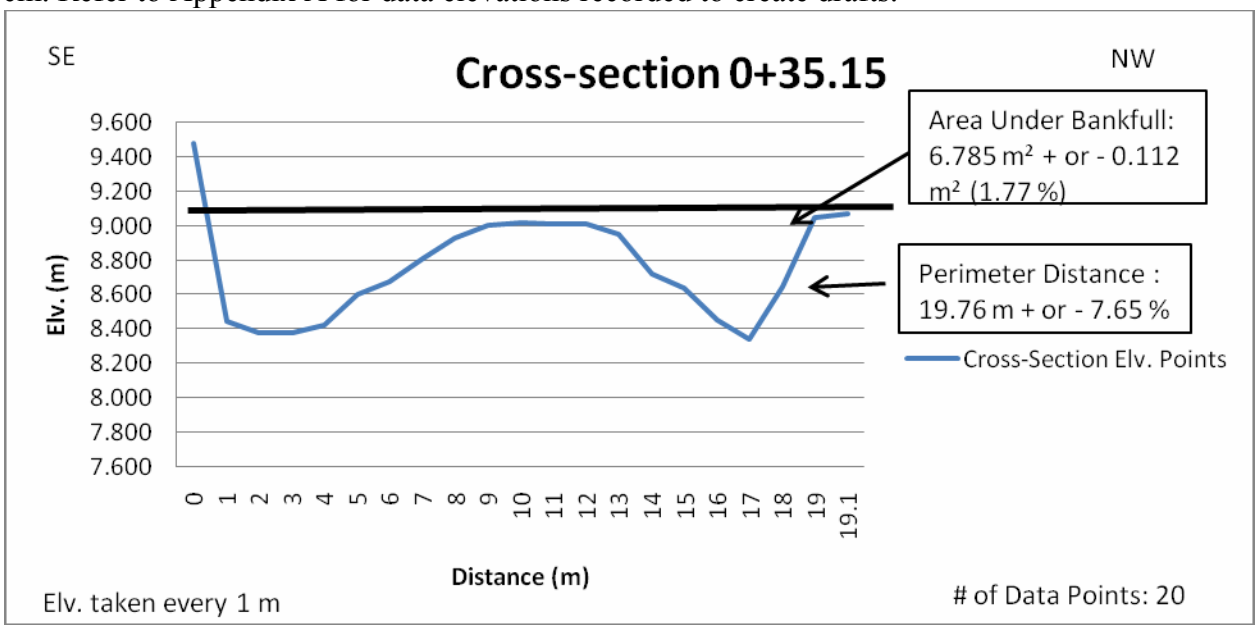

Figure 6: b) Graph of the same data but only using elevation data at every 1 meter increments from 0-19.1. Refer to Appendix A for data elevations recorded to create drafts.

*Water surface elevation Surveys***:**

The water surface elevation was surveyed at low flow and bankfull stage in order to obtain channel gradient, which is an important component in a stream's shear stress because it represents the major force being applied due to gravity. Although they are important, gradient measurements were the hardest variable to determine. Gradients were low and varied significantly between high and low flows. The plan was to take gradient measurement throughout the gravel bar section being measured. Water surface elevations will be used to calculate the gradient.

*Grain Size Measurements***:**

The method used for collecting a grain size distribution is to walk a grid pattern on the gravel bar selecting random grain sizes at the top/base of your foot. (Wolman, 1954). To find an accurate value for the 84 % size grain it was suggested that 100 + grain size samples were to be recorded. Surface Grain size data for the channels, gravel bar and on banks were collected separately. I measured surface grain sizes at each channel cross section (see appendix). In many cases the two sides of the channel had different grain size distributions, therefore, I measured each side of the channel separately. The central gravel bar also had a different grain size distribution than the channels, so it was also measured separately.

Data Analyses:

For this project, I surveyed 8 channel cross sections, measured 12 channel grain size distributions and 3 bar grain size distributions. Channel bed slope and water surface gradient were surveyed at low flow and water surface gradient was surveyed again after a bankfull flood event that occurred in February, 2008. From these data I determined: depth distribution in each channel cross section; grain size distribution in each channel cross section, and local bankfull gradient for each channel cross section (for each distributary channel separately in locations where the channel was divided). From these morphological and grain size data, I then determined average boundary shear stress for each cross section, and dimensionless shear stress values for each cross section. I also generated shear stress distributions across the channel for each location.

RESULTS:

In Table I: I show the channel morophology and grain size parameters for the cross section averaged data for each of the sites. Analysis of survey error indicates a 2% error in the measurement of channel depths and channel areas.

TABLE I: Cross Section Averages of Morphological and Grain size data

(Cross Section Averages Tables)

Site	Distance	Station #	Depth	Width	W/d	D84	depth/d84	Gradient
1	0	(neg)-0+11	0.65	19.41	29.862	0.0710	9.1549	0.0145
2	11	0+00	0.559	16.38	29.302	0.0663	8.4314	0.0145
3	17.7	0+6.7	0.472	14.71	31.165	0.0686	6.8805	0.0145
4	35	0+24	0.862	12.75	14.791	0.0630	13.6825	0.0145
5	46.15	0+35.15	0.302	19.14	63.377	0.0606	4.9835	0.0223
6	57.7	0+46.7	0.445	27.5	61.798	0.0557	7.9892	0.0225
7	71.9	0+60.9	0.765	24.4	31.895	0.0613	12.4796	0.0228
8	97	0+86	0.783	21.1	26.948	0.0658	11.8997	0.0222

Cross Section Average Channel Morphology

The cross-section average data for channel morphology is shown in figure 7. In these diagrams the reach without a central bar extends from distances 0-35 m downstream; The gravel bar extends from 35-80 m downstream, and the channel forms a single thread in distances 80-97 m downstream.

The overall shallowest average depths are present in the gravel bar reach. Depth is a large factor in the ability of bedload transport. The shallower average depths have significant effects which lower the overall applied shear stress to the gravel size particles. The width to depth rate also increases significantly at the head of the channel bar, but returns to a similar value downstream of the bar. Within the gravel bar the reach of the stream the width depth ratio varies considerably and could indicate possible stability of the gravel bar complex.

From the cross-section surveys I was able to visually represent the changes in the streams morphology as it incountered the gravel bar my interest. The graphs created and shown in Appendix B also show the migration of the channel from starting as a left side dominate channel to a right side dominate channel. The channel surveys were used to determine depths across the channel to use as a factor in determining dimensionless shear stress. Figure 6 represents the average depths at each channel profile through the 100 meter analization of the stresam. The average depth is highly varient throughout the gravel bar reagion of the stream.

-

a)

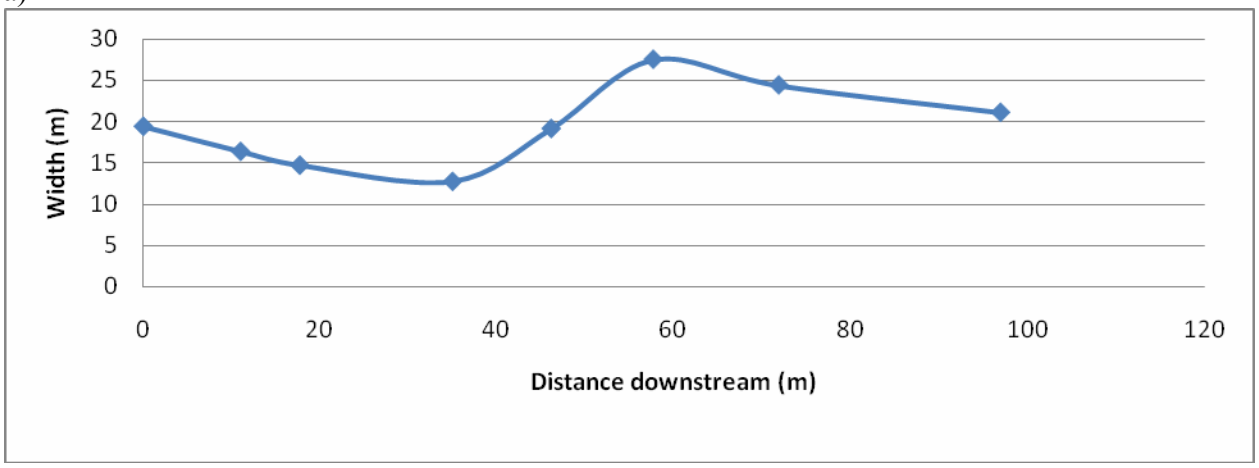

b)

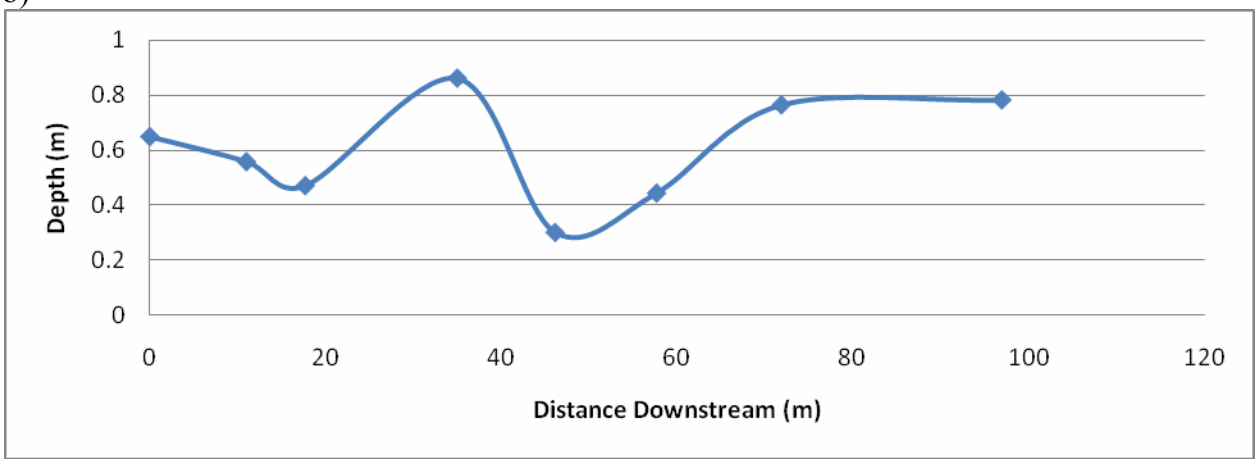

c)

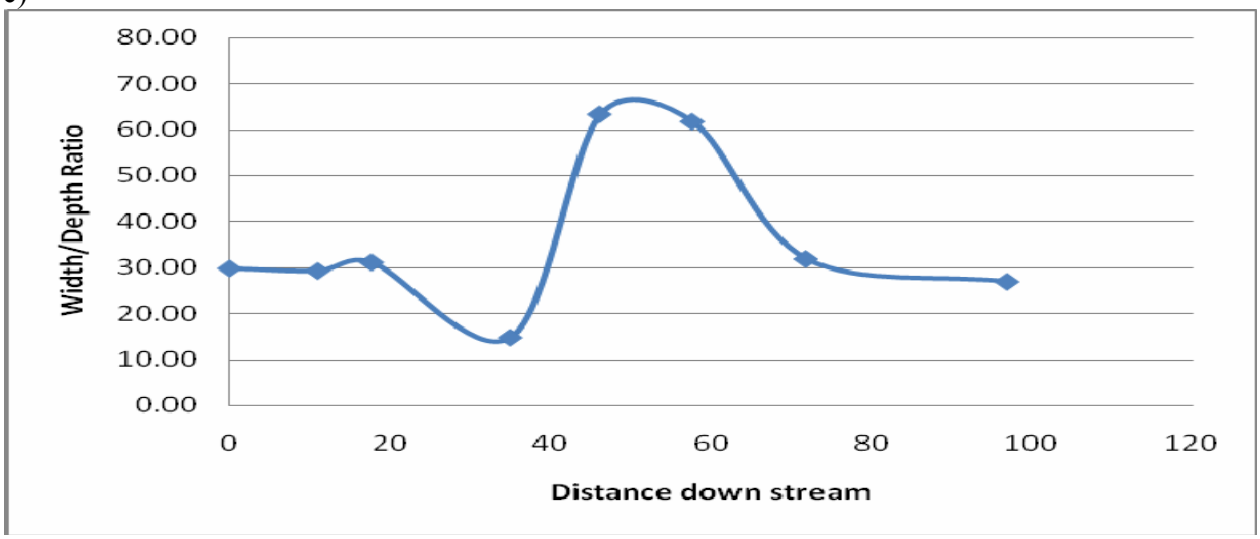

Figure 7: a) Graph of width changes downstream. The width of the stream becomes the narrowest prior to the gravel bar formation. Width of stream is re-established to initial width once passing the gravel bar reach of the stream. b) Graph of average depth changes downstream.

Bankfull Flow and Low Flow Water Surface Gradient

Water surface gradients were measured during low flow, and bankfull events. The low flow and bankfull gradients through the reach are shown in fig. 8. Gradient measurments were probably the hardest measurements to record. Graident data can be found in Apendix D. These measurments had to be recorded during high flows. Initally I measured surfacewater elevations during high flows. Then I then decided later that marking the elevation of the suface water with a flag and coming back at a later date to record elevations was more efficent. The high flow gradients were similar to the low flow gradients for one of the channels, only the dominant channel was measured at low flow and it also had the steepest gradient at high flow. In this channel, the water surface gradient was significantly higher in the braided reach than in the upstream area. This has been seen in other studies of braided reaches (Leopold et al., 1964). I determined that high flows did have a higher energy graident then low flows, but not significantly different. The Energy gradient was determined twice to be steeper on the left side of the channel compared to the right side of the channel at the gravel bar complex, this is represented in Figure 8. I took the different gradients into consideration when calculating dimensionless shear stress. Note that the increase in water surface gradient through the reach somewhat offsets the decrease in channel depth.

Grain Size Distribution Data

The D_{84} from each sample was determined from the graphs grain size distribution. These data were combined to evaluate average grain size distribution in the channel at each cross section location. In general, the grain sizes do not change over the reach (fig. 9), but this is somethwat misleading, because the grain sizes on the mid-channel bar are much smaller than in the two distributary channels. From the graphs, the gravel bar contained the smallest grain sizes, with banks being the next largest and channel bed containing the largest grain sizes found in the stream. The gravel bar grain size samples shown in Figure 10 are interesting because as the gravel bar decends down stream the grain size becomes smaller. This is illistraded in Figure 10.

The average grain size data for a cross section were not used to determine critical dimensionless shear stress values. Rather, at each cross section, grain size data were evaluated separately for each of the two channels and the central bar. For example, at cross-section station # 0+47 (57.7 meters downstream), which was the larges cross-section of the stream, used four different grain sizes to calculate the dimensionless shear stress arcoss the change. Figure 9 essential depict that the overall grain size throughout the cross-section are relatively similar throught this part of the PBS. The largest average grain sizes coincide with the largest depths of the stream which is what would be expected.

a)

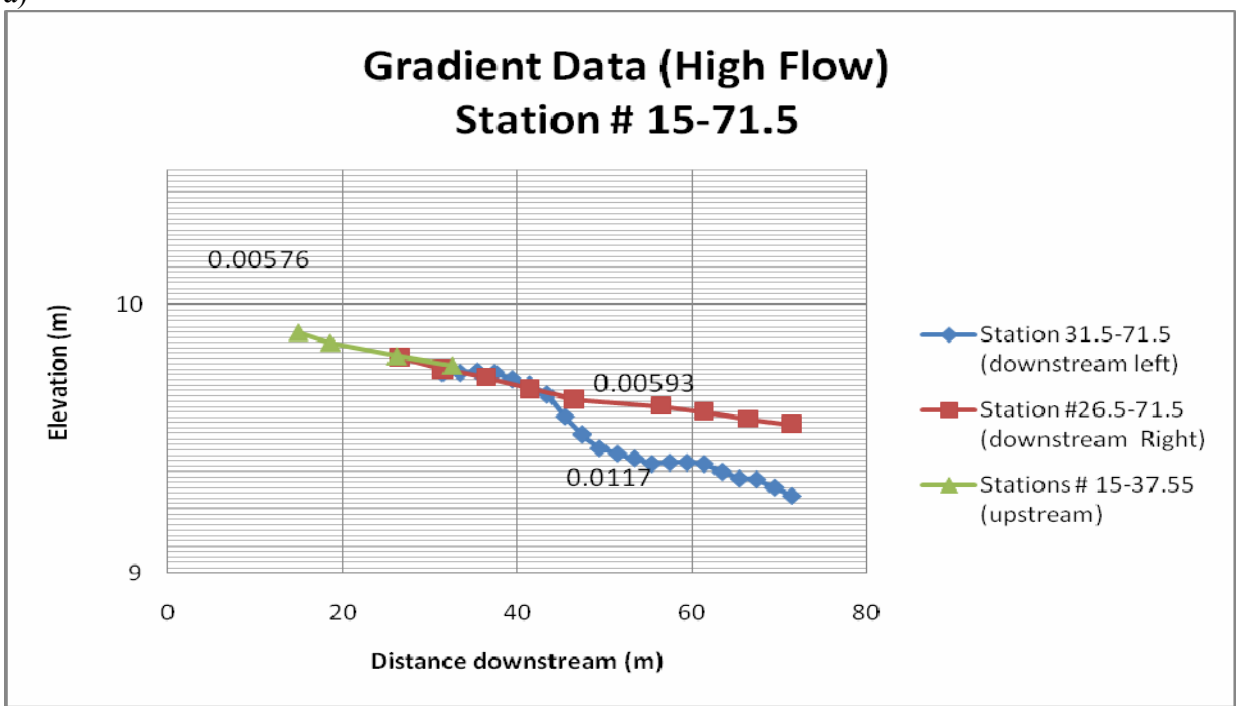

b)

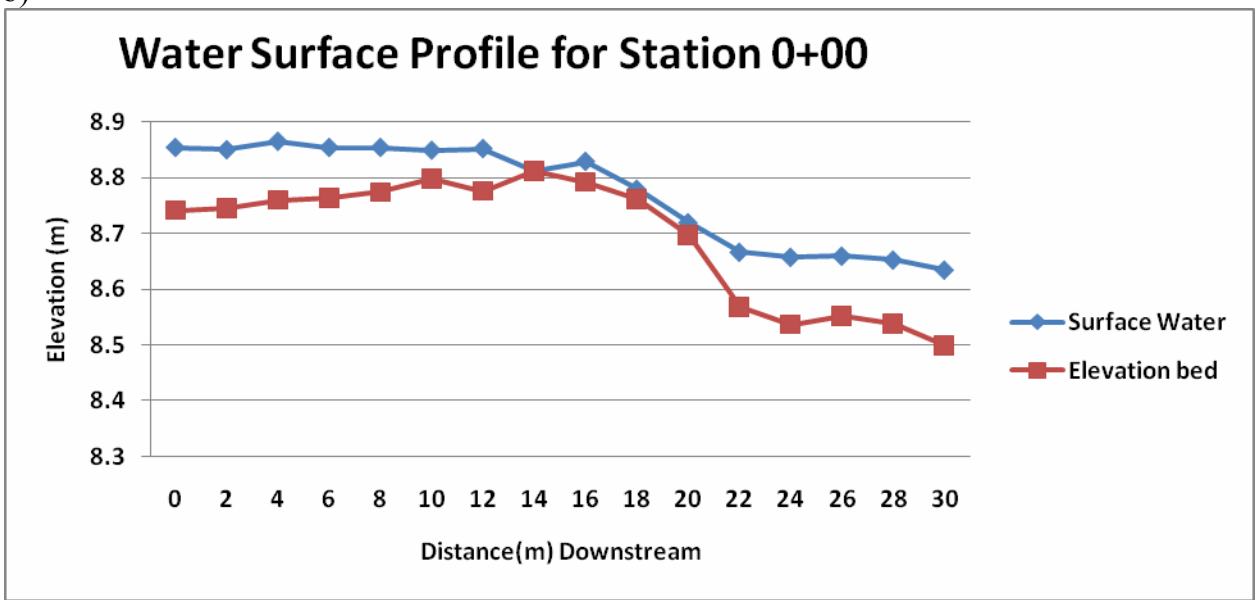

Figure 8: a) Represents the gradients at high flows (upper diagram) and b) low flow (lower diagram). The gravel bar splits the channel into two separate channels. These two channel experence two different energy gradients. From the graph you can see the right channel remains a relitively similar gradient to the energy

Channel D84 vs. Distance Downstream

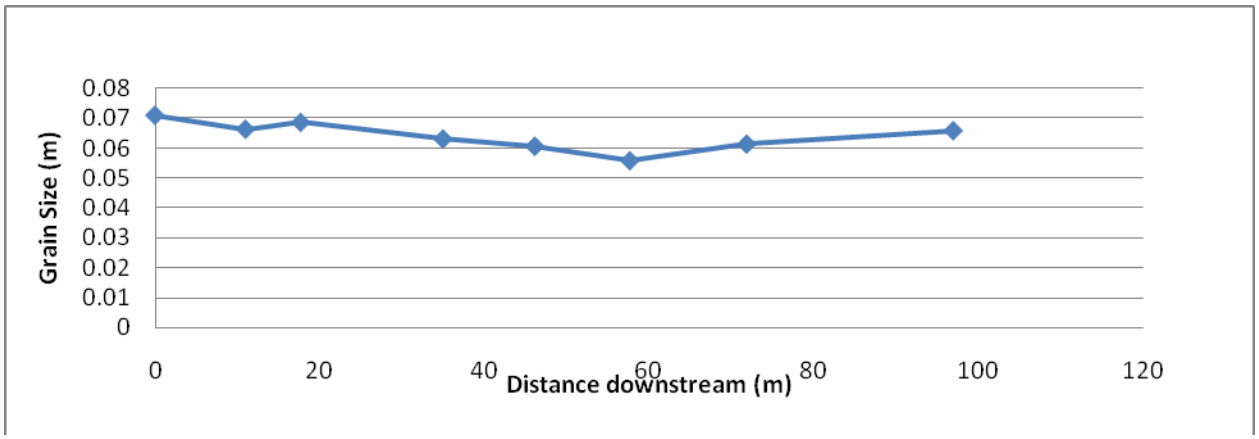

Figure 9: Graph represents the changes in average grain size throughout the channel. The graph shows that the average D84 grain size remains overall consistant throughout the region of stream research.

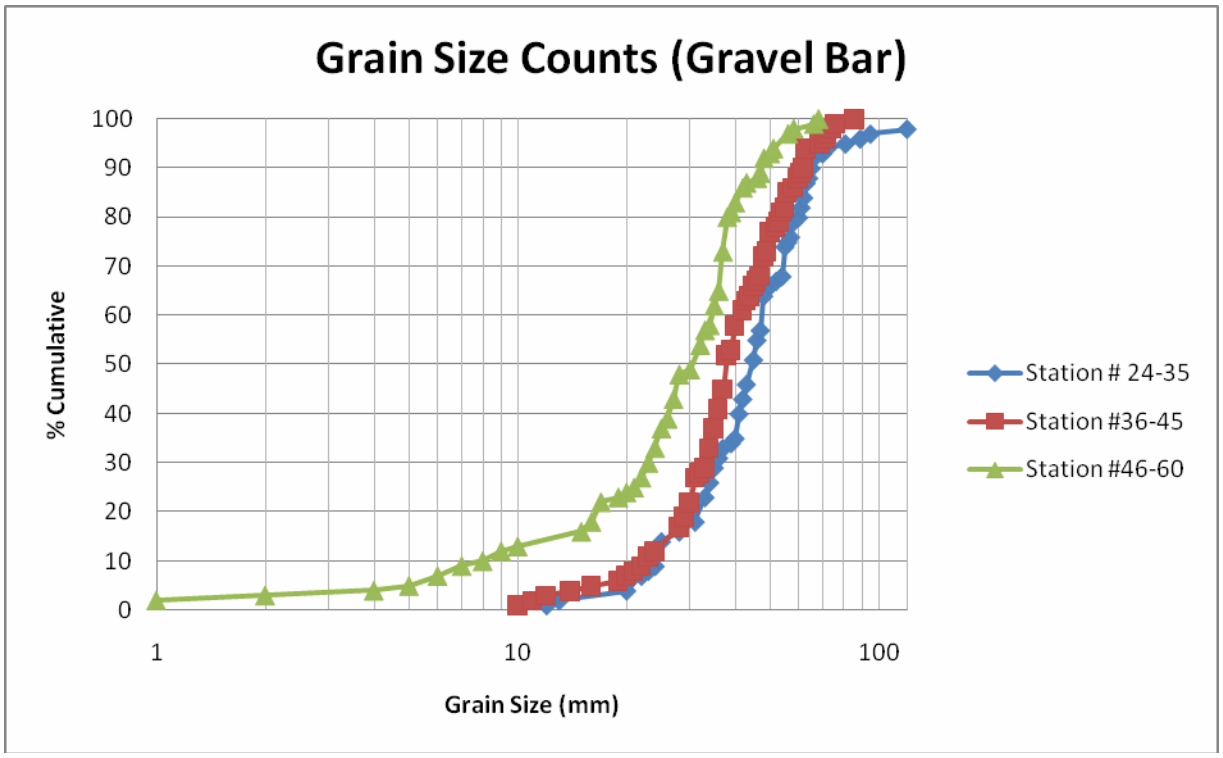

Figure 10: This graph is a representation of 3 gavel sediment distributions taken from the gravel bar. Station # 24-35 distribution is a sample from the initial formation of the gravel bar. The gravel size particals decrease in average size as the gravel bar elongates down stream.

Dimensionless Shear Stress Distribution

Eight dimensionless shear stress graphs were created, one for each cross section (Appendix E). These eight graphs incorporated the three variables collected grain size, gradient and depth. As grain size changed along the profile of the channel I used an average grain size sample distribution that was collected in that location. Some graphs utilized 4 different grain size distributions across the channel. The cross channel shear stresses distributions in the Appendix showed several things: the lowest bed shear stresses at bankfull stage were over the gravel bar and along the banks, indicating that at bankfull stage, the gravel bar and the stream banks are relatively stable features. The downstream changes in dimensionless shear stress are shown in Table II, and on figure 11. The red line on the diagram of the dimensionless shear stress graphs represents the critical dimensionless shear stress for bedload transport. Points above the line represent areas in which total bed movement of gravel size particles would move. Below the red line represents areas in which are considered stable with no movement at bank-full conditions.
This diagram indicate that the channel downstream of the bar, where depths are high, width is relatively low, and gradient is relatively high, results in the highest shear stresses downstream of the channel bar, which is where further channel change, such as widening might occur.

Table II: Dimensioless Shear Stress Values.

Site	Dimensionless Shear Stress	(T-T*crit (0.045))= Excess Shearstress
1	0.0706	0.0256
2	0.0598	0.0148
3	0.0369	0.000
4	0.0992	0.0542
5	0.0511	0.0061
6	0.0956	0.0506
7	0.1627	0.1177
8	0.1425	0.0975

Channel cross-section profiles with the smallest average dimensionless shear stress.

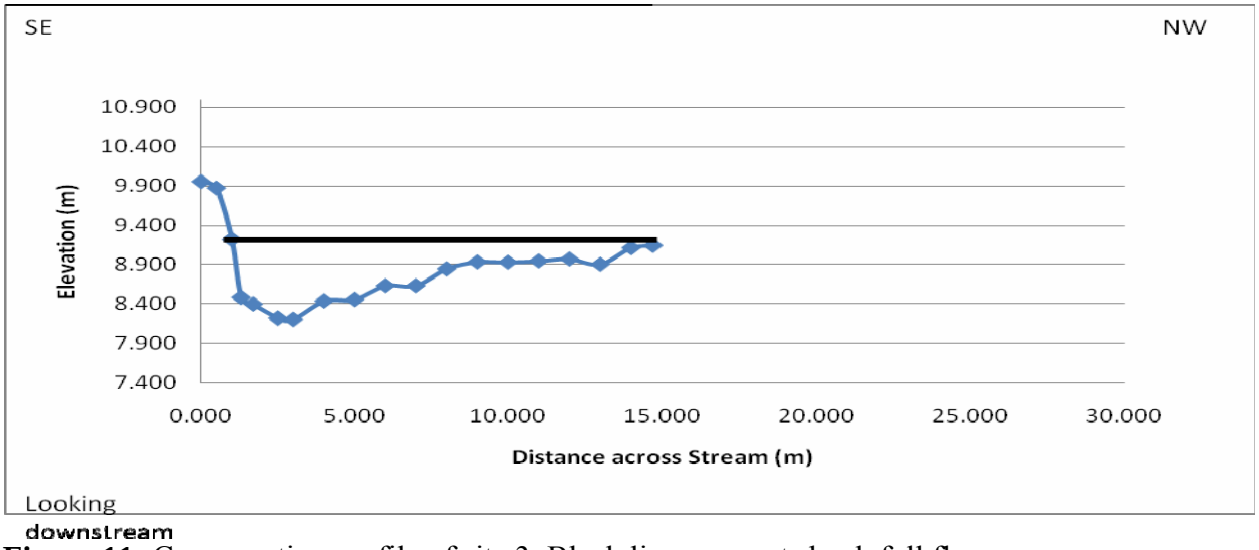

Figure 11: Cross-section profile of site 3. Black line represnts bank full flow.

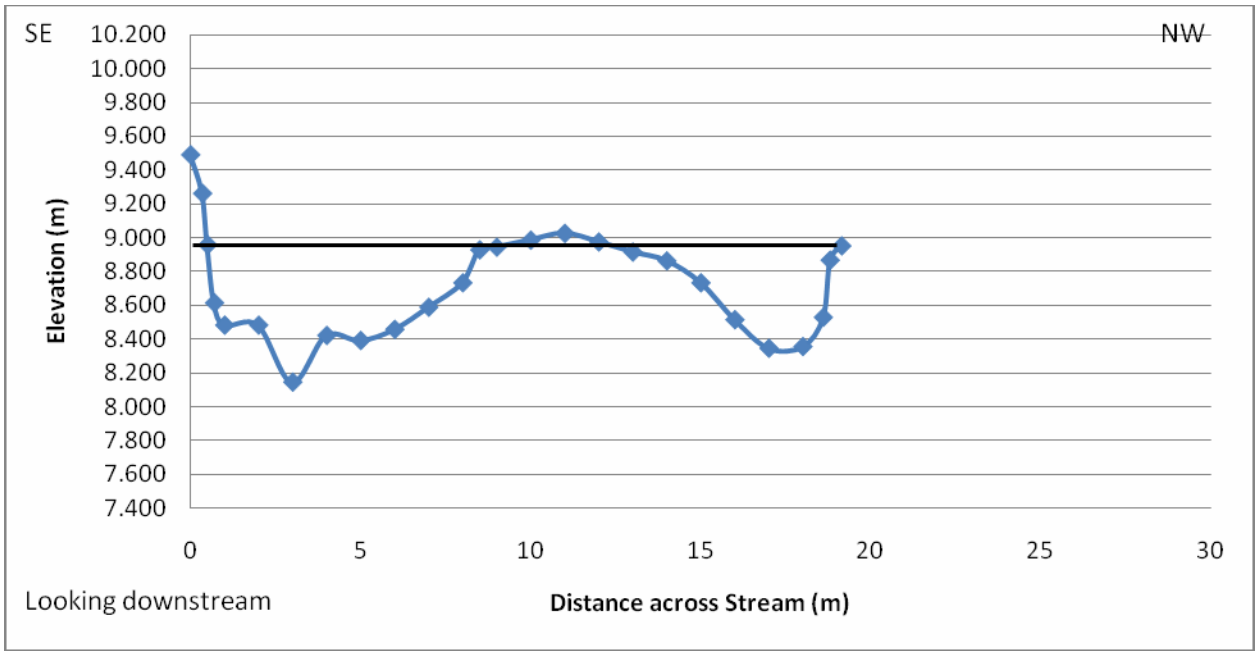

Figure 12: Cross-section profile of site 5. Black line represents bank full flow.

Figure 11 (site 3) and 12 (site 5) are the two croos-section profiles that dimensionless shear stress if close to or below the critical dimensionless shear stress. Both of these areas are considered to be stable according to Shields dimensionless shear stress equation. Whats interesting is that these two cross sections are vastly different. Figure 11 is a cross section prior to the gravel bar with a relatively small width and depth. Site 5 is a cross section that is 10 m into the gravel bar complex with a larger width and even smaller depths across the channel. Compared to site 3, site

5 has two channels separated by the gravel bar. The gravel bar elevations in site 5 was recorded to be the same elevation as the top of the banks, this is illistraded by the black line in fig. 12.

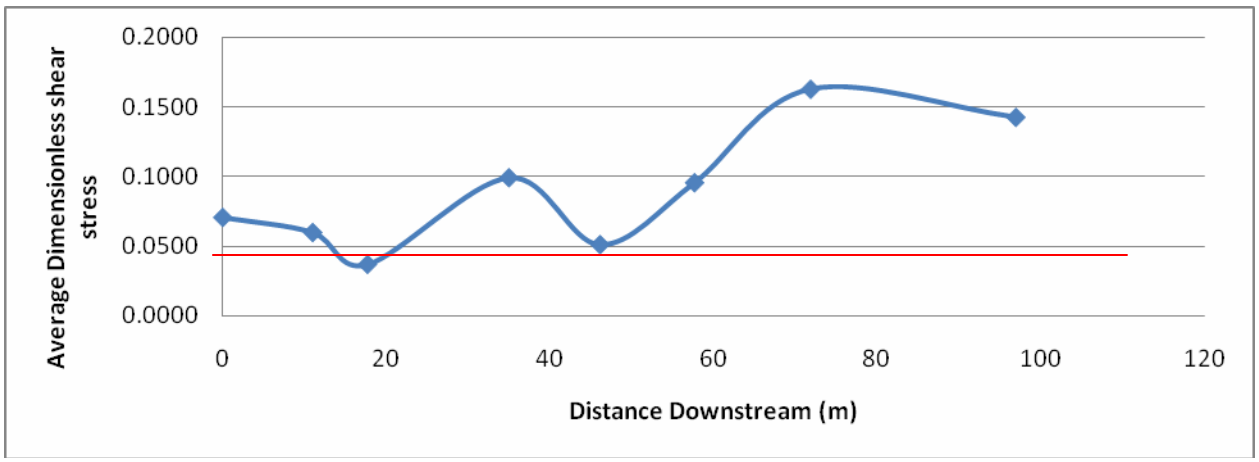

Figure 13: Graph represent the average shear stress at each cross-section of the channel as the morphology changes downstream. In corralation with Figure 9 the graph represents the locations where shear stress is mininumun.

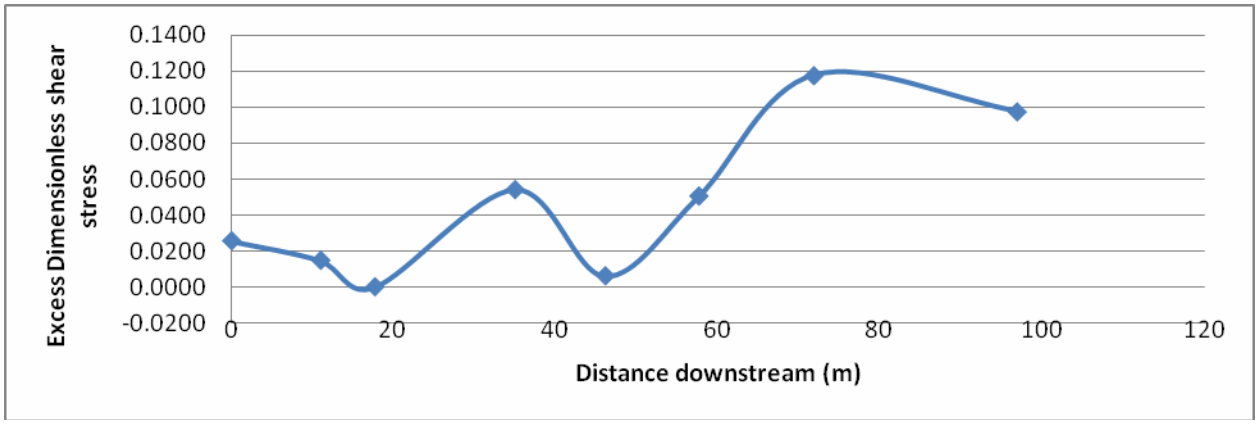

Figure 14: Graph represents the average excess shear stress present at each cross-section downstream. There are two locations where the excess shear stress is 0, both regions are where the gravel bar is present.

Figure 14 correlates to Figure 13 to show the potential excess shear stress to within the channel throughout the section of PBS analyzed. There are two areas in which excess shear stress is zero of very minimum. These two areas, located at 20 and 50 meters distance downstream, are sections in which the gravel bar starts to form. This is interesting because the gravel bar is not entirely stable throughout the entire complex do to the excess shear stress presented between 20 and 50 meters downstream. Currently the gravel bar is not completely stable. I hypothesize that overtime the gravel bar will become completely stable throughout based on Sheild dimensionless shear stress criterian.

Conclusions:

1. The morphological data indicate that the channel widens considerably at the entrance to the gravel bar reach, but then the channel width decreases downstream to a value similar to the initial width.

2. The total average grain size, distributed within each cross section does not change significantly downstream through the bar complex. However, within the gravel bar section, the sediment on the bar is much finer grained than the sediment within the channel. Thus the stream has sorted the bedload material so that the fine material is stored in the channel bar.

3. The channel gradient increases over the section of the reach that contains the gravel bar, but one side of the channel has a much higher gradient than the other.

4. Dimensionless shear stress values are not significantly different between the upstream straight reach and the top of the gravel bar, but shear stress values are highest at the downstream end of the bar.

5. Cross channel dimensionless shear stress distributions indicate that the channel banks and the channel bar are both near or below the threshold of motion.

Bibliography:

Barry, J., 2004. A general power equation for predicting bed load transport rates in gravel bed rivers, *Water Resources Research*, 40, W10401.

Buffington, J. M., and D. R. Montgomery, 1997. A systematic analysis of eight decades of incipient motion studies, with special reference to gravel bedded rivers, *Water Resources Research*, 1993-2029.

Constantine, C. R., Mount, J. F., and Florsheim, 2003. The Effects of Longitudinal Differences in Gravel Mobility on the Downstream Fining Pattern in the Cosumnes River, California, *The Journal of Geology*, 111, 233-241.

Dietrich, W. E., Kirchner, J. W., Ikeda, H., and Iseya. F., 1989. Sediment supply and the development of the coarse surface layer in gravel-bedded rivers, *Nature*, 340, 215-217.

Goodwin, P., 2004. Analytical Solution for Estimating Effective Discharge, *Journal of hydraulic Engineering,*130, 8, 729-728.

Hjulstrom, F. (1939) Transportation of detritus by moving water. *In Recent Marine Sediments. A Symposium,* edited by P.Trask. Tulsa,OK: Am Assoc. Petroleum Geologists..

Miller, M. C., McCave, I. N. and Komar, P. D., 1997. Threshold of sediment motion under unidirectional currents, *Sedimentology*, 24, 507-527.

Parker, G., 1978. Self-formed straight rivers with equilibrium banks and mobile bed Part 2. The gravel river. *Journal of Fluid Mechanics*, vol. 89, p.127-146.

Renger, F., and Wohl, E., 2007. Trends of grain sizes on gravel bars in the Rio Chagres, Panama, *Geomorphology*, 83, 282-293.

Ritter, D. F., Kochel, C. R., & Miller, J. R., 2002. *Process Geomorphology* (4th ed.). Long Grove, Illinois: Waveland Press.

Shields, A., 1936. Application of similarity principles and turbulence research to bed-load movement. California Inst. Tech., W.M Keck Lab. *Of Hydraulics and Water Resources*, Rept. No.167.

Wiberg, P. L. Smith, J. D., 1989. Erodibility of coarse, poorly sorted sediment American. Geophysical Union: Washington, DC, United States, 70, 15, 321.

Wilson, K. C., 2005. Rapid Increase in Suspended Load at High Bed Shear, *Journal of Hydraulic Engineering*, 131, 1, 46-51.

Appendix A: (Error Data) Figure: 4 (a) Data at Cross-section #0+35.15

Date: 11-3-07	Weather: 55, sunny	Time: 11:00 am	*BF width (m)= 19.1*

Cherry Hill Road upstream of 1st Bar	Station # 0+35.15 m	ELV-10.000 m = Edge of Path near tree

Distance (m)	*Backsite (m)*	*H.I.*	*Foresite depth. (m)*	*Elevation (m)*	*Area (m^2)*	*Mat*	*Perimeter Distance*
0.00	0.750	10.750	1.268	9.482	-0.021		0.051
0.05			1.280	9.470	-0.020		0.050
0.10			1.273	9.477	-0.020		0.057
0.15			1.301	9.449	-0.019		0.055
0.20			1.278	9.472	-0.020		0.055
0.25			1.302	9.448	-0.019		0.158
0.30			1.452	9.298	-0.011		0.054
0.35			1.473	9.277	-0.010		0.078
0.40			1.533	9.217	-0.007		0.135
0.45			1.658	9.092	-0.001		0.153
0.50			1.803	8.947	0.006		0.065
0.55			1.845	8.905	0.008		0.100
0.60			1.932	8.818	0.013		0.161
0.65			2.085	8.665	0.020		0.052
0.70			2.098	8.652	0.021		0.096
0.75			2.180	8.570	0.025		0.069
0.80			2.228	8.522	0.027		0.050
0.85			2.235	8.515	0.028		0.053
0.90			2.253	8.497	0.029		0.054
0.95			2.273	8.477	0.030		0.057
1.00			2.301	8.449	0.031		0.063
1.05			2.339	8.411	0.033		0.050
1.10			2.339	8.411	0.033		0.050
1.15			2.339	8.411	0.033		0.052
1.20			2.325	8.425	0.032		0.050
1.25			2.325	8.425	0.032		0.050
1.30			2.332	8.418	0.033		0.050
1.35			2.328	8.422	0.032		0.051
1.40			2.338	8.412	0.033		0.050
1.45			2.338	8.412	0.033		0.050

1.50			2.345	8.405	0.033		0.050
1.55			2.343	8.407	0.033		0.052
1.60			2.358	8.392	0.034		0.050
1.65			2.352	8.398	0.034		0.051
1.70			2.363	8.387	0.034		0.050
1.75			2.366	8.384	0.034		0.050
1.80			2.365	8.385	0.034		0.050
1.85			2.366	8.384	0.034		0.050
1.90			2.361	8.389	0.034		0.050
1.95			2.365	8.385	0.034		0.050
2.00			2.368	8.382	0.034		0.050
2.05			2.364	8.386	0.034		0.051
2.10			2.352	8.398	0.034		0.050
2.15			2.350	8.400	0.034		0.051
2.20			2.360	8.390	0.034		0.050
2.25			2.360	8.390	0.034		0.050
2.30			2.355	8.395	0.034		0.050
2.35			2.356	8.394	0.034		0.050
2.40			2.354	8.396	0.034		0.050
2.45			2.353	8.397	0.034		0.052
2.50			2.368	8.382	0.034		0.050
2.55			2.368	8.382	0.034		0.050
2.60			2.372	8.378	0.035		0.051
2.65			2.362	8.388	0.034		0.050
2.70			2.368	8.382	0.034		0.050
2.75			2.375	8.375	0.035		0.054
2.80			2.355	8.395	0.034		0.051
2.85			2.366	8.384	0.034		0.050
2.90			2.365	8.385	0.034		0.051
2.95			2.373	8.377	0.035		0.050
3.00			2.371	8.379	0.035		0.050
3.05			2.374	8.376	0.035		0.050
3.10			2.377	8.373	0.035		0.053
3.15			2.359	8.391	0.034		0.052
3.20			2.375	8.375	0.035		0.114
3.25			2.273	8.477	0.030		0.086
3.30			2.343	8.407	0.033		0.050
3.35			2.344	8.406	0.033		0.054
3.40			2.323	8.427	0.032		0.063
3.45			2.361	8.389	0.034		0.050
3.50			2.362	8.388	0.034		0.050

3.55			2.360	8.390	0.034		0.050
3.60			2.366	8.384	0.034		0.050
3.65			2.373	8.377	0.035		0.051
3.70			2.383	8.367	0.035		0.055
3.75			2.361	8.389	0.034		0.050
3.80			2.355	8.395	0.034		0.050
3.85			2.359	8.391	0.034		0.059
3.90			2.328	8.422	0.032		0.050
3.95			2.332	8.418	0.033		0.051
4.00			2.324	8.426	0.032		0.050
4.05			2.325	8.425	0.032		0.051
4.10			2.335	8.415	0.033		0.056
4.15			2.310	8.440	0.032		0.054
4.20			2.290	8.460	0.031		0.055
4.25			2.268	8.482	0.029		0.050
4.30			2.267	8.483	0.029		0.053
4.35			2.250	8.500	0.029		0.051
4.40			2.260	8.490	0.029		0.050
4.45			2.255	8.495	0.029		0.050
4.50			2.258	8.492	0.029		0.052
4.55			2.245	8.505	0.028		0.051
4.60			2.235	8.515	0.028		0.054
4.65			2.215	8.535	0.027		0.055
4.70			2.238	8.512	0.028		0.054
4.75			2.258	8.492	0.029		0.050
4.80			2.255	8.495	0.029		0.053
4.85			2.238	8.512	0.028		0.061
4.90			2.203	8.547	0.026		0.050
4.95			2.202	8.548	0.026		0.074
5.00			2.148	8.602	0.023		0.071
5.05			2.198	8.552	0.026		0.051
5.10			2.190	8.560	0.026		0.050
5.15			2.188	8.562	0.025		0.053
5.20			2.170	8.580	0.025		0.053
5.25			2.151	8.599	0.024		0.051
5.30			2.163	8.587	0.024		0.050
5.35			2.165	8.585	0.024		0.055
5.40			2.142	8.608	0.023		0.050
5.45			2.148	8.602	0.023		0.050
5.50			2.142	8.608	0.023		0.050
5.55			2.148	8.602	0.023		0.050

5.60			2.145	8.605	0.023		0.053
5.65			2.128	8.622	0.022		0.050
5.70			2.128	8.622	0.022		0.054
5.75			2.108	8.642	0.021		0.050
5.80			2.102	8.648	0.021		0.052
5.85			2.088	8.662	0.020		0.050
5.90			2.082	8.668	0.020		0.051
5.95			2.073	8.677	0.020		0.050
6.00			2.073	8.677	0.020		0.050
6.05			2.078	8.672	0.020		0.050
6.10			2.079	8.671	0.020		0.050
6.15			2.072	8.678	0.020		0.050
6.20			2.068	8.682	0.019		0.053
6.25			2.050	8.700	0.019		0.050
6.30			2.048	8.702	0.018		0.051
6.35			2.040	8.710	0.018		0.050
6.40			2.035	8.715	0.018		0.052
6.45			2.021	8.729	0.017		0.063
6.50			1.982	8.768	0.015		0.051
6.55			1.973	8.777	0.015		0.050
6.60			1.978	8.772	0.015		0.050
6.65			1.976	8.774	0.015		0.050
6.70			1.973	8.777	0.015		0.050
6.75			1.968	8.782	0.014		0.050
6.80			1.970	8.780	0.015		0.050
6.85			1.969	8.781	0.014		0.056
6.90			1.995	8.755	0.016		0.080
6.95			1.932	8.818	0.013		0.050
7.00			1.935	8.815	0.013		0.050
7.05			1.933	8.817	0.013		0.052
7.10			1.918	8.832	0.012		0.057
7.15			1.890	8.860	0.011		0.050
7.20			1.892	8.858	0.011		0.053
7.25			1.873	8.877	0.010		0.050
7.30			1.868	8.882	0.009		0.055
7.35			1.845	8.905	0.008		0.052
7.40			1.832	8.918	0.008		0.050
7.45			1.830	8.920	0.008		0.054
7.50			1.810	8.940	0.007		0.050
7.55			1.812	8.938	0.007		0.054
7.60			1.832	8.918	0.008		0.050

7.65			1.838	8.912	0.008		0.050
7.70			1.838	8.912	0.008		0.050
7.75			1.839	8.911	0.008		0.050
7.80			1.839	8.911	0.008		0.050
7.85			1.838	8.912	0.008		0.050
7.90			1.840	8.910	0.008		0.051
7.95			1.829	8.921	0.007		0.052
8.00			1.815	8.935	0.007		0.050
8.05			1.812	8.938	0.007		0.050
8.10			1.808	8.942	0.006		0.051
8.15			1.800	8.950	0.006		0.050
8.20			1.802	8.948	0.006		0.050
8.25			1.803	8.947	0.006		0.050
8.30			1.805	8.945	0.006		0.050
8.35			1.798	8.952	0.006		0.050
8.40			1.798	8.952	0.006		0.050
8.45			1.802	8.948	0.006		0.050
8.50			1.798	8.952	0.006		0.052
8.55			1.784	8.966	0.005		0.050
8.60			1.784	8.966	0.005		0.050
8.65			1.789	8.961	0.005		0.050
8.70			1.787	8.963	0.005		0.050
8.75			1.786	8.964	0.005		0.050
8.80			1.785	8.965	0.005		0.050
8.85			1.779	8.971	0.005		0.052
8.90			1.765	8.985	0.004		0.050
8.95			1.758	8.992	0.004		0.051
9.00			1.747	9.003	0.003		0.051
9.05			1.759	8.991	0.004		0.050
9.10			1.758	8.992	0.004		0.050
9.15			1.756	8.994	0.004		0.052
9.20			1.742	9.008	0.003		0.056
9.25			1.768	8.982	0.004		0.050
9.30			1.772	8.978	0.005		0.051
9.35			1.781	8.969	0.005		0.050
9.40			1.782	8.968	0.005		0.050
9.45			1.775	8.975	0.005		0.050
9.50			1.771	8.979	0.005		0.050
9.55			1.766	8.984	0.004		0.051
9.60			1.758	8.992	0.004		0.050
9.65			1.755	8.995	0.004		0.050

9.70			1.749	9.001	0.003		0.050
9.75			1.742	9.008	0.003		0.050
9.80			1.737	9.013	0.003		0.050
9.85			1.731	9.019	0.003		0.050
9.90			1.729	9.021	0.002		0.050
9.95			1.730	9.020	0.003		0.050
10.00			1.732	9.018	0.003		0.050
10.05			1.735	9.015	0.003		0.050
10.10			1.742	9.008	0.003		0.051
10.15			1.730	9.020	0.003		0.050
10.20			1.736	9.014	0.003		0.050
10.25			1.737	9.013	0.003		0.052
10.30			1.722	9.028	0.002		0.051
10.35			1.733	9.017	0.003		0.052
10.40			1.720	9.030	0.002		0.051
10.45			1.728	9.022	0.002		0.051
10.50			1.716	9.034	0.002		0.052
10.55			1.730	9.020	0.003		0.050
10.60			1.728	9.022	0.002		0.050
10.65			1.729	9.021	0.002		0.050
10.70			1.722	9.028	0.002		0.050
10.75			1.718	9.032	0.002		0.050
10.80			1.721	9.029	0.002		0.050
10.85			1.717	9.033	0.002		0.050
10.90			1.719	9.031	0.002		0.053
10.95			1.737	9.013	0.003		0.050
11.00			1.735	9.015	0.003		0.050
11.05			1.732	9.018	0.003		0.050
11.10			1.728	9.022	0.002		0.050
11.15			1.726	9.024	0.002		0.050
11.20			1.730	9.020	0.003		0.054
11.25			1.750	9.000	0.004		0.050
11.30			1.752	8.998	0.004		0.050
11.35			1.750	9.000	0.004		0.050
11.40			1.750	9.000	0.004		0.050
11.45			1.746	9.004	0.003		0.050
11.50			1.750	9.000	0.004		0.051
11.55			1.742	9.008	0.003		0.052
11.60			1.758	8.992	0.004		0.050
11.65			1.753	8.997	0.004		0.050
11.70			1.751	8.999	0.004		0.052

11.75			1.738	9.012	0.003		0.052
11.80			1.751	8.999	0.004		0.050
11.85			1.751	8.999	0.004		0.050
11.90			1.748	9.002	0.003		0.051
11.95			1.740	9.010	0.003		0.050
12.00			1.734	9.016	0.003		0.051
12.05			1.742	9.008	0.003		0.051
12.10			1.753	8.997	0.004		0.051
12.15			1.743	9.007	0.003		0.051
12.20			1.753	8.997	0.004		0.052
12.25			1.766	8.984	0.004		0.050
12.30			1.760	8.990	0.004		0.052
12.35			1.773	8.977	0.005		0.052
12.40			1.758	8.992	0.004		0.052
12.45			1.773	8.977	0.005		0.050
12.50			1.768	8.982	0.004		0.050
12.55			1.773	8.977	0.005		0.050
12.60			1.775	8.975	0.005		0.050
12.65			1.768	8.982	0.004		0.052
12.70			1.783	8.967	0.005		0.050
12.75			1.782	8.968	0.005		0.050
12.80			1.783	8.967	0.005		0.050
12.85			1.783	8.967	0.005		0.051
12.90			1.791	8.959	0.006		0.050
12.95			1.794	8.956	0.006		0.050
13.00			1.792	8.958	0.006		0.050
13.05			1.796	8.954	0.006		0.050
13.10			1.796	8.954	0.006		0.050
13.15			1.794	8.956	0.006		0.050
13.20			1.788	8.962	0.005		0.051
13.25			1.796	8.954	0.006		0.050
13.30			1.798	8.952	0.006		0.050
13.35			1.805	8.945	0.006		0.050
13.40			1.810	8.940	0.007		0.060
13.45			1.843	8.907	0.008		0.051
13.50			1.852	8.898	0.009		0.054
13.55			1.872	8.878	0.010		0.057
13.60			1.900	8.850	0.011		0.053
13.65			1.918	8.832	0.012		0.051
13.70			1.928	8.822	0.012		0.052
13.75			1.942	8.808	0.013		0.059

13.80			1.973	8.777	0.015		0.051
13.85			1.983	8.767	0.015		0.052
13.90			1.999	8.751	0.016		0.051
13.95			2.010	8.740	0.017		0.052
14.00			2.024	8.726	0.017		0.052
14.05			2.039	8.711	0.018		0.051
14.10			2.049	8.701	0.018		0.051
14.15			2.060	8.690	0.019		0.051
14.20			2.070	8.680	0.020		0.051
14.25			2.080	8.670	0.020		0.051
14.30			2.092	8.658	0.021		0.051
14.35			2.101	8.649	0.021		0.050
14.40			2.102	8.648	0.021		0.050
14.45			2.109	8.641	0.021		0.050
14.50			2.112	8.638	0.022		0.050
14.55			2.113	8.637	0.022		0.050
14.60			2.113	8.637	0.022		0.050
14.65			2.117	8.633	0.022		0.050
14.70			2.117	8.633	0.022		0.050
14.75			2.112	8.638	0.022		0.050
14.80			2.107	8.643	0.021		0.050
14.85			2.102	8.648	0.021		0.050
14.90			2.108	8.642	0.021		0.050
14.95			2.108	8.642	0.021		0.050
15.00			2.110	8.640	0.022		0.050
15.05			2.115	8.635	0.022		0.050
15.10			2.108	8.642	0.021		0.050
15.15			2.105	8.645	0.021		0.053
15.20			2.123	8.627	0.022		0.050
15.25			2.124	8.626	0.022		0.052
15.30			2.111	8.639	0.022		0.050
15.35			2.114	8.636	0.022		0.061
15.40			2.149	8.601	0.023		0.051
15.45			2.141	8.609	0.023		0.050
15.50			2.138	8.612	0.023		0.051
15.55			2.150	8.600	0.024		0.050
15.60			2.155	8.595	0.024		0.054
15.65			2.175	8.575	0.025		0.051
15.70			2.187	8.563	0.025		0.057
15.75			2.215	8.535	0.027		0.053
15.80			2.232	8.518	0.028		0.053

15.85			2.251	8.499	0.029		0.055
15.90			2.273	8.477	0.030		0.051
15.95			2.285	8.465	0.030		0.051
16.00			2.293	8.457	0.031		0.050
16.05			2.298	8.452	0.031		0.051
16.10			2.308	8.442	0.031		0.050
16.15			2.308	8.442	0.031		0.059
16.20			2.340	8.410	0.033		0.050
16.25			2.343	8.407	0.033		0.050
16.30			2.350	8.400	0.034		0.051
16.35			2.358	8.392	0.034		0.050
16.40			2.352	8.398	0.034		0.060
16.45			2.385	8.365	0.035		0.153
16.50			2.240	8.510	0.028	Log	0.065
16.55			2.198	8.552	0.026	Log	0.050
16.60			2.195	8.555	0.026	Log	0.200
16.65			2.389	8.361	0.035		0.050
16.70			2.387	8.363	0.035		0.050
16.75			2.389	8.361	0.035		0.055
16.80			2.411	8.339	0.037		0.050
16.85			2.408	8.342	0.036		0.050
16.90			2.403	8.347	0.036		0.050
16.95			2.409	8.341	0.036		0.050
17.00			2.405	8.345	0.036		0.051
17.05			2.415	8.335	0.037		0.050
17.10			2.420	8.330	0.037		0.067
17.15			2.465	8.285	0.039		0.054
17.20			2.485	8.265	0.040		0.050
17.25			2.479	8.271	0.040		0.051
17.30			2.469	8.281	0.039		0.058
17.35			2.440	8.310	0.038		0.053
17.40			2.422	8.328	0.037		0.050
17.45			2.420	8.330	0.037		0.052
17.50			2.405	8.345	0.036		0.051
17.55			2.413	8.337	0.037		0.052
17.60			2.398	8.352	0.036		0.050
17.65			2.395	8.355	0.036		0.055
17.70			2.372	8.378	0.035		0.078
17.75			2.312	8.438	0.032		0.050
17.80			2.305	8.445	0.031		0.053
17.85			2.323	8.427	0.032		0.209

17.90			2.120	8.630	0.022		0.051
17.95			2.112	8.638	0.022		0.052
18.00			2.098	8.652	0.021		0.050
18.05			2.104	8.646	0.021		0.052
18.10			2.117	8.633	0.022		0.052
18.15			2.130	8.620	0.023		0.053
18.20			2.149	8.601	0.023		0.055
18.25			2.173	8.577	0.025		0.050
18.30			2.174	8.576	0.025		0.050
18.35			2.177	8.573	0.025		0.088
18.40			2.105	8.645	0.021		0.054
18.45			2.085	8.665	0.020		0.099
18.50			2.000	8.750	0.016		0.168
18.55			1.840	8.910	0.008		0.139
18.60			1.970	8.780	0.015		0.155
18.65			1.823	8.927	0.007		0.074
18.70			1.769	8.981	0.004		0.058
18.75			1.740	9.010	0.003		0.051
18.80			1.732	9.018	0.003		0.118
18.85			1.839	8.911	0.008		0.053
18.90			1.821	8.929	0.007		0.133
18.95			1.698	9.052	0.001		0.050
19.00			1.700	9.050	0.001		0.052
19.05			1.685	9.065	0.000		0.050
19.10			1.680	9.070	0.000		
				Total Area:	6.907	Perimeter	21.393

Appendix A (continued): (Error Data) Figure: 4 (b) Data at Cross-section #0+35.15

Variability Data			Same values as heavily measured on at every (m) rather then (0.05) m				
Date: 11-3-07		Weather: 55, sunny		Time: 11:00 am		*BF width (m)=19.1*	
Cherry Hill Road upstream of 1st Bar			Station # 0+35.15 m		ELV-10.000 m = Edge of Path near tree		
Distance (m)	*Backsite (m)*	*H.I.*	*Foresite depth. (m)*	*Elevation (m)*	*Area (m^2)*	*Mat*	*Perimeter Distance*
0	0.75	10.75	1.268	9.482	-0.412		1.438
1			2.301	8.449	0.621		1.002
2			2.368	8.382	0.688		1.000
3			2.371	8.379	0.691		1.001
4			2.324	8.426	0.644		1.015
5			2.148	8.602	0.468		1.003
6			2.073	8.677	0.393		1.009
7			1.935	8.815	0.255		1.007
8			1.815	8.935	0.135		1.002
9			1.747	9.003	0.067		1.000
10			1.732	9.018	0.052		1.000
11			1.735	9.015	0.055		1.000
12			1.734	9.016	0.054		1.002
13			1.792	8.958	0.112		1.027
14			2.024	8.726	0.344		1.004
15			2.110	8.640	0.430		1.017
16			2.293	8.457	0.613		1.006
17			2.405	8.345	0.725		1.046
18			2.098	8.652	0.418		1.076
19			1.700	9.050	0.020		0.102
19.1			1.680	9.070	0.000		
				Total Area	6.785	Total Perimeter:	19.757

Appendix B: Cross-Section Data #1,2,3,4,5,6,7 & 8

Cross-Section Graphs created using Data:

1)

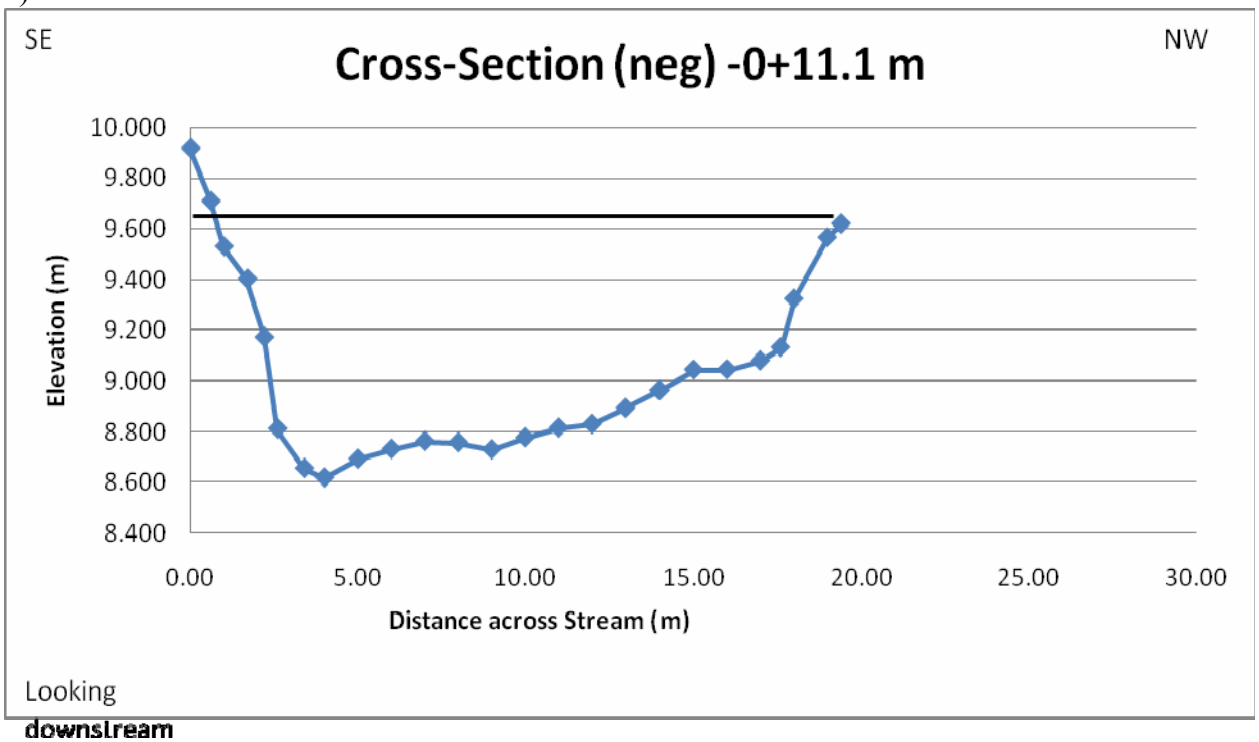

2)

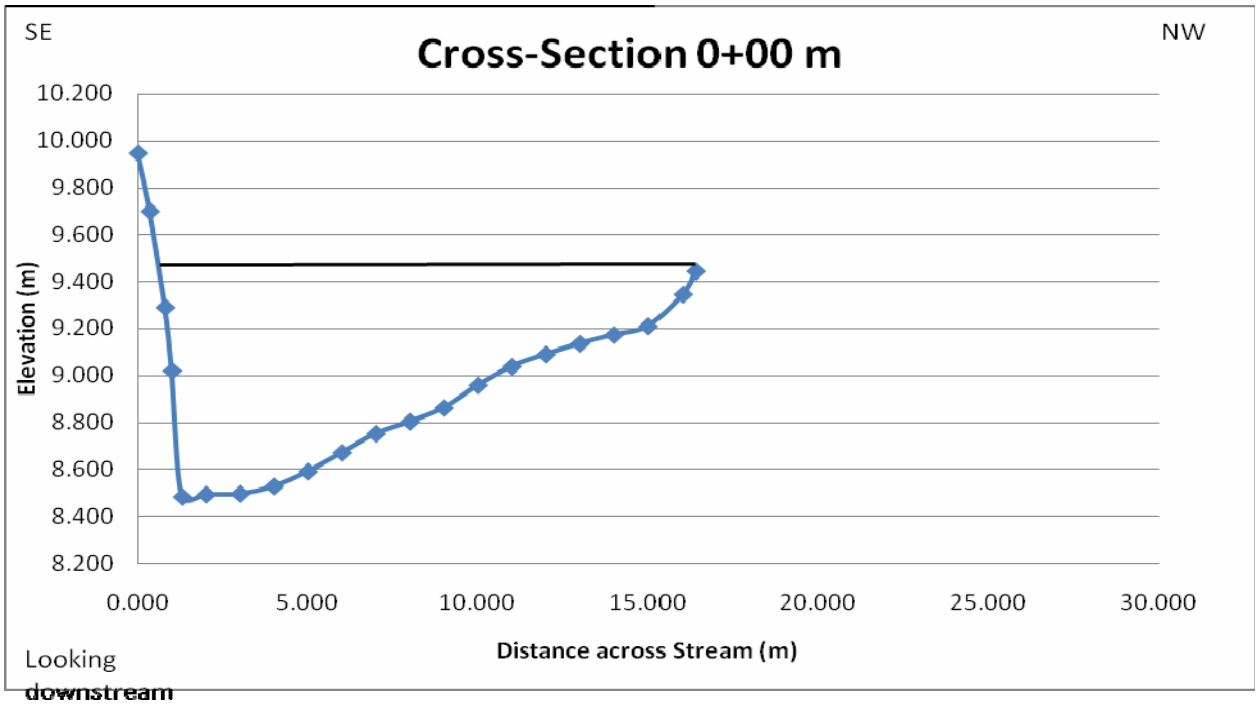

3)

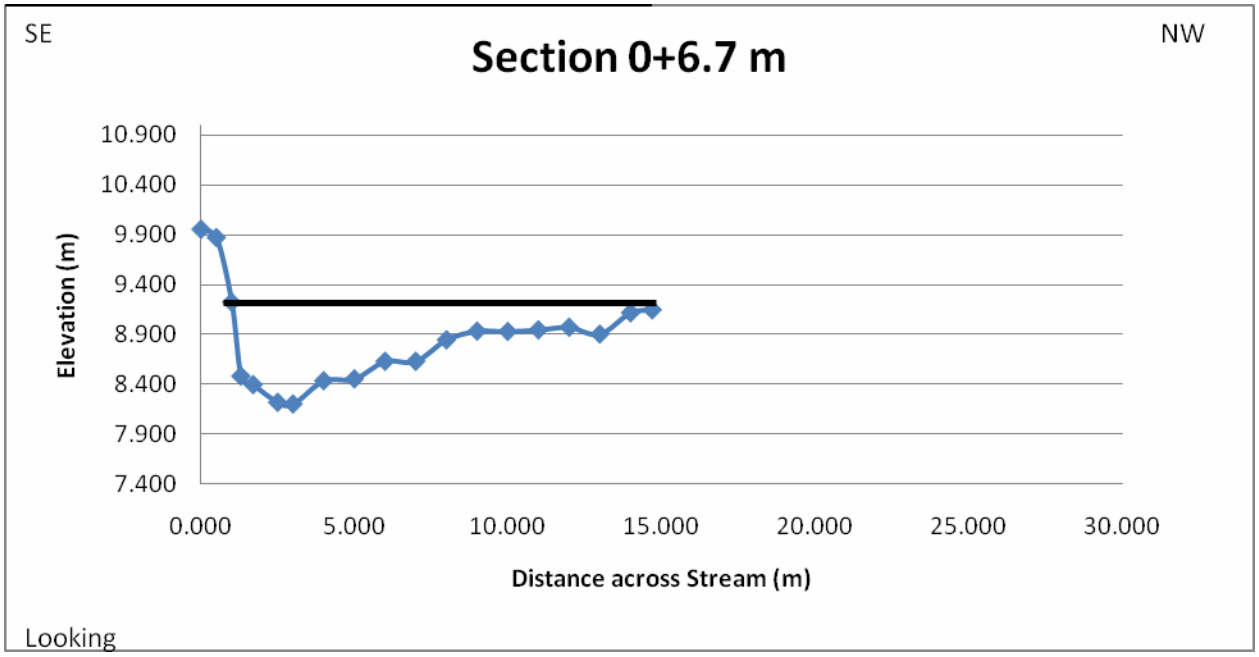
SE
NW
Section 0+6.7 m
10.900
10.400
9.900
9.400
8.900
8.400
7.900
7.400
Elevation (m)
0.000
5.000
10.000
15.000
20.000
25.000
30.000
Distance across Stream (m)
Looking
downstream

4)

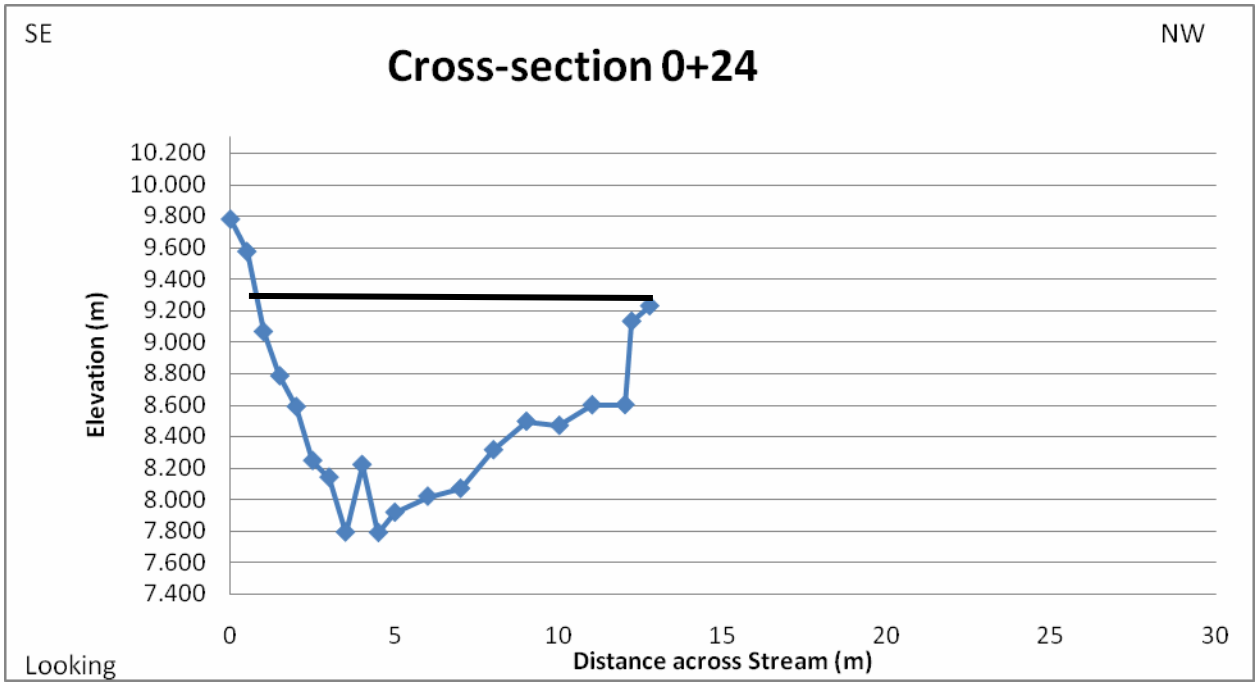
SE
NW
Cross-section 0+24
10.200
10.000
9.800
9.600
9.400
9.200
9.000
8.800
8.600
8.400
8.200
8.000
7.800
7.600
7.400
Elevation (m)
0
5
10
15
20
25
30
Distance across Stream (m)
Looking
downstream

5)

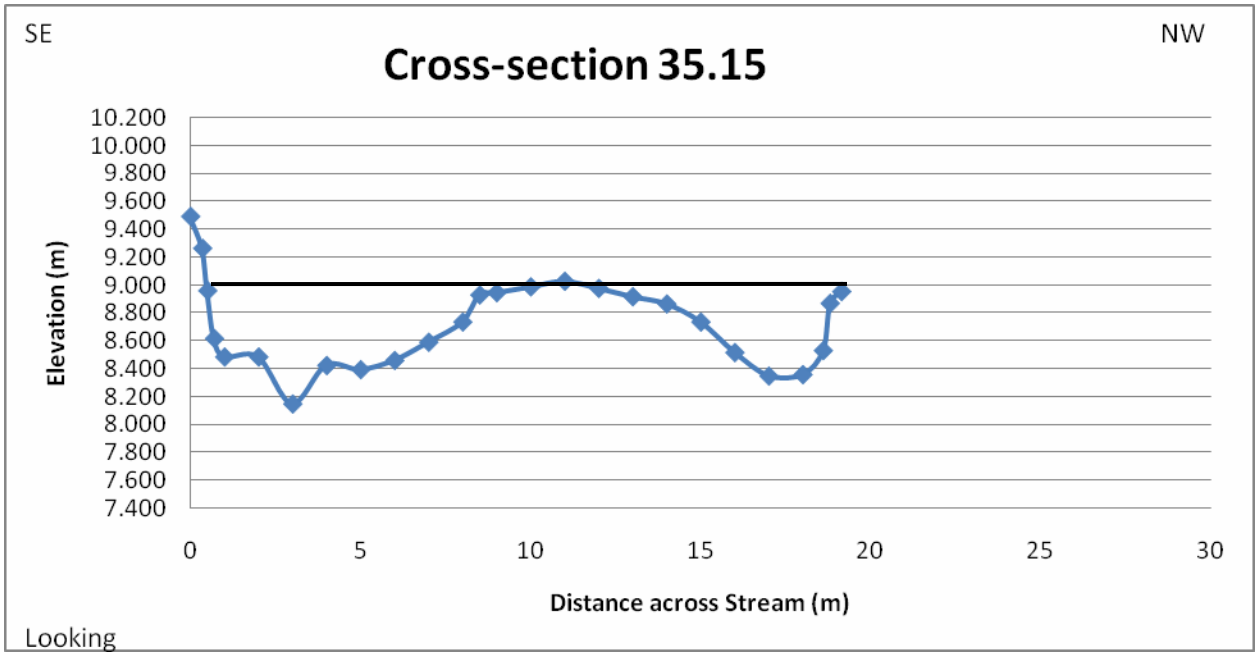
SE
NW
Cross-section 35.15
10.200
10.000
9.800
9.600
9.400
9.200
9.000
8.800
8.600
8.400
8.200
8.000
7.800
7.600
7.400
Elevation (m)
0
5
10
15
20
25
30
Distance across Stream (m)
Looking downstream

6)

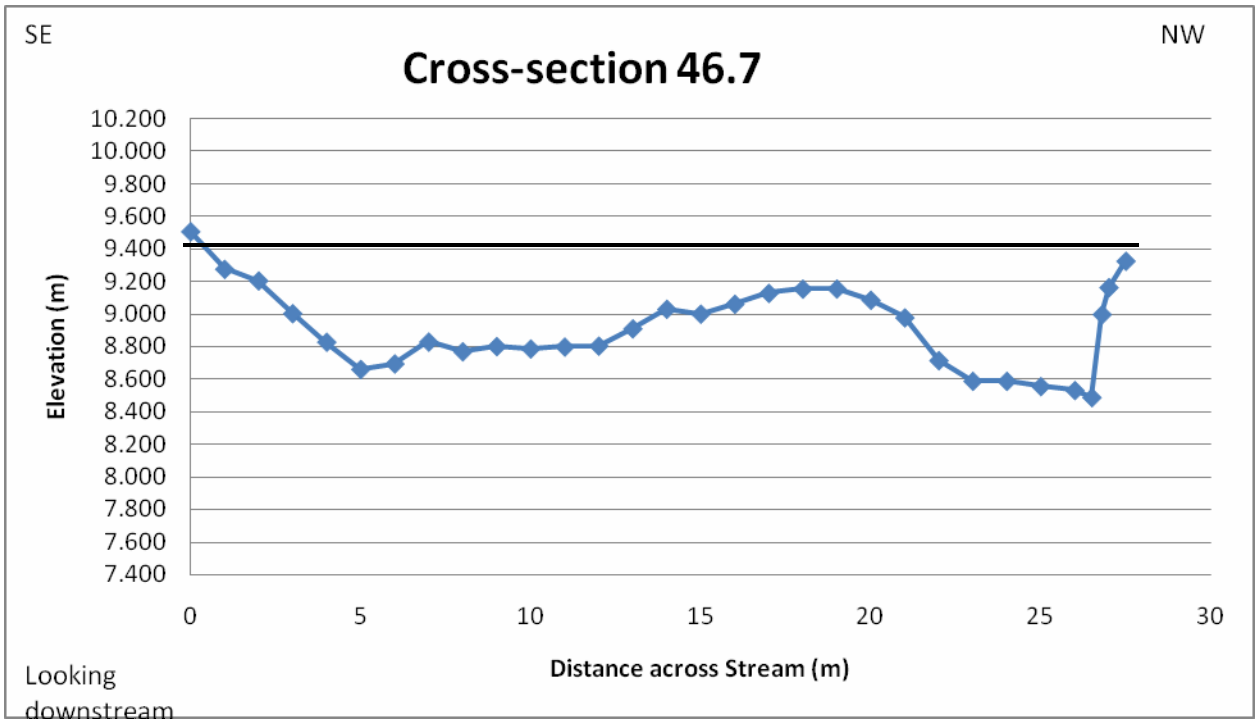
SE
NW
Cross-section 46.7
10.200
10.000
9.800
9.600
9.400
9.200
9.000
8.800
8.600
8.400
8.200
8.000
7.800
7.600
7.400
Elevation (m)
0
5
10
15
20
25
30
Distance across Stream (m)
Looking downstream

7)

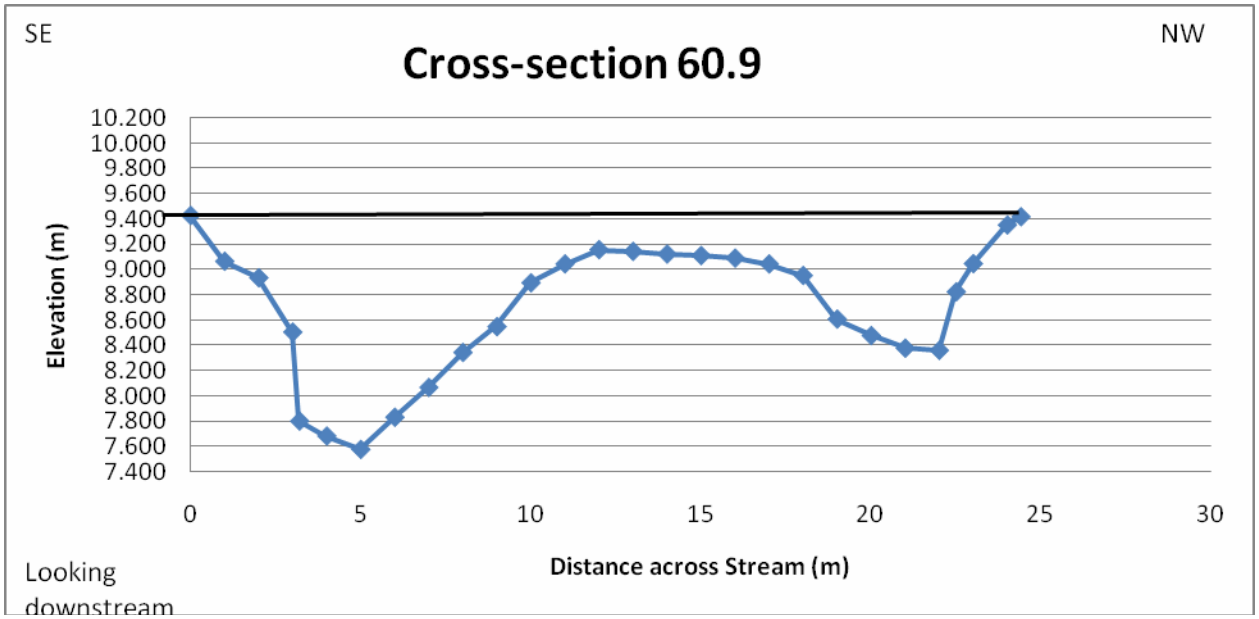
SE
NW
Cross-section 60.9
10.200
10.000
9.800
9.600
9.400
9.200
9.000
8.800
8.600
8.400
8.200
8.000
7.800
7.600
7.400
Elevation (m)
0
5
10
15
20
25
30
Distance across Stream (m)
Looking downstream

8)

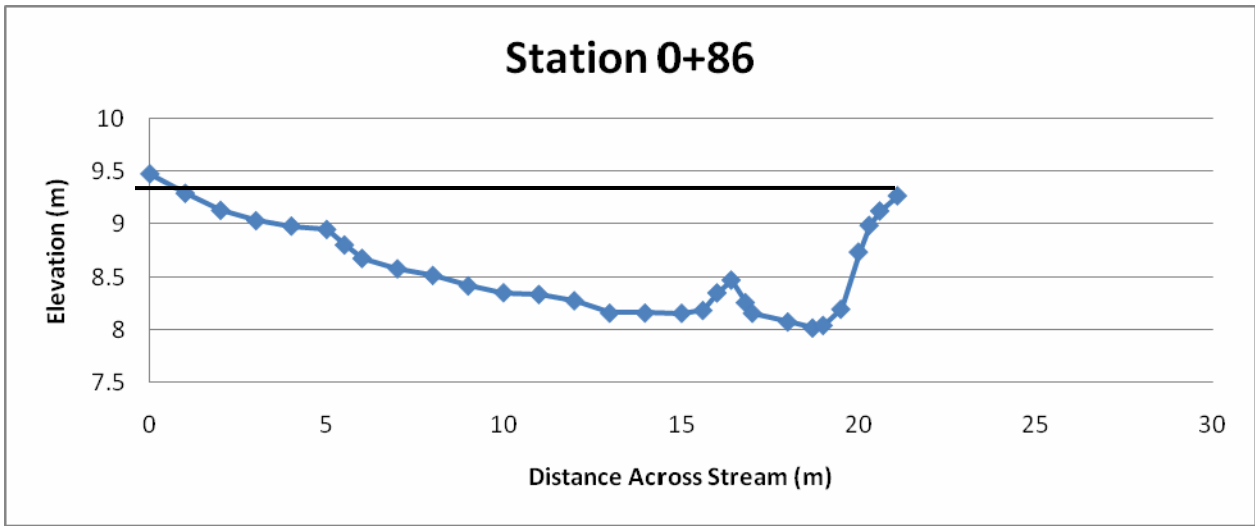
Station 0+86
10
9.5
9
8.5
8
7.5
Elevation (m)
0
5
10
15
20
25
30
Distance Across Stream (m)

Appendix C: Grain Size Distributions #1,2,3,4,5,6,7,8,9,10

Gravel Distributions gravels at location throughout stream:

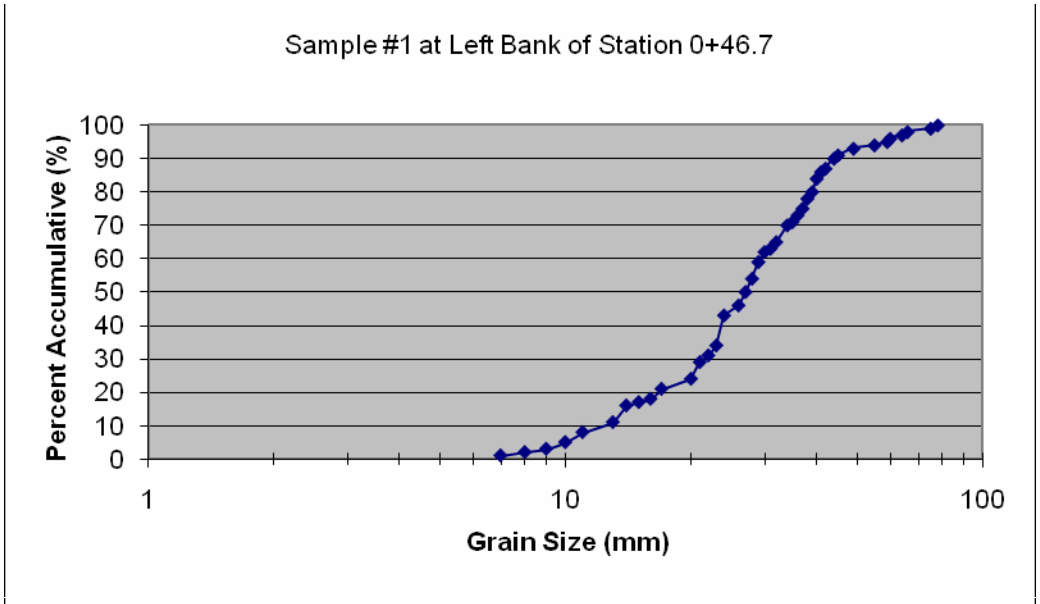

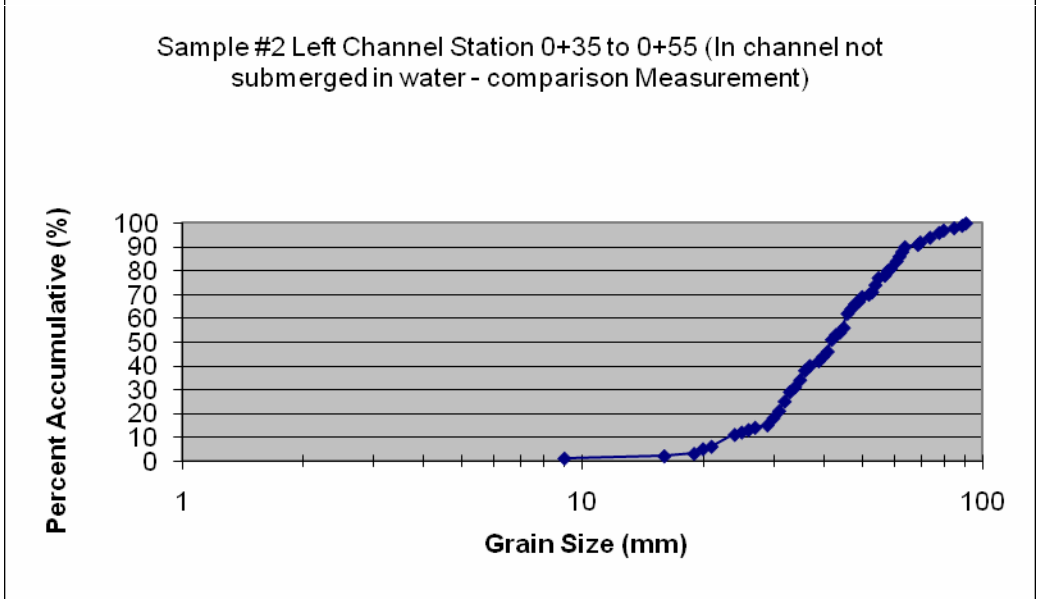

Sample #3 Station 0+00 to 0+11 Gravel Bar Up-Stream

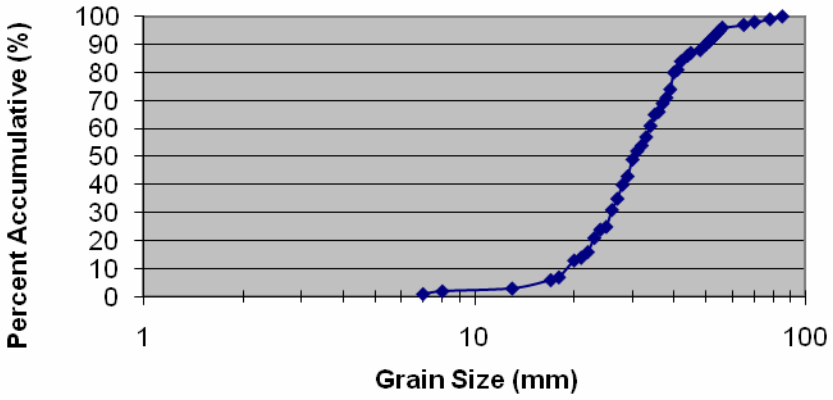

Sample #4 Stations -0+11 to 0+00 Gravel Bar Up- Stream

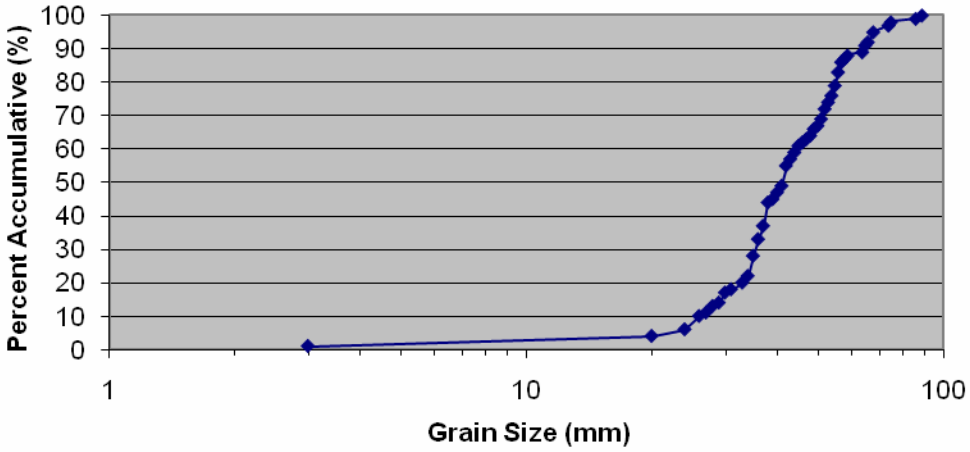

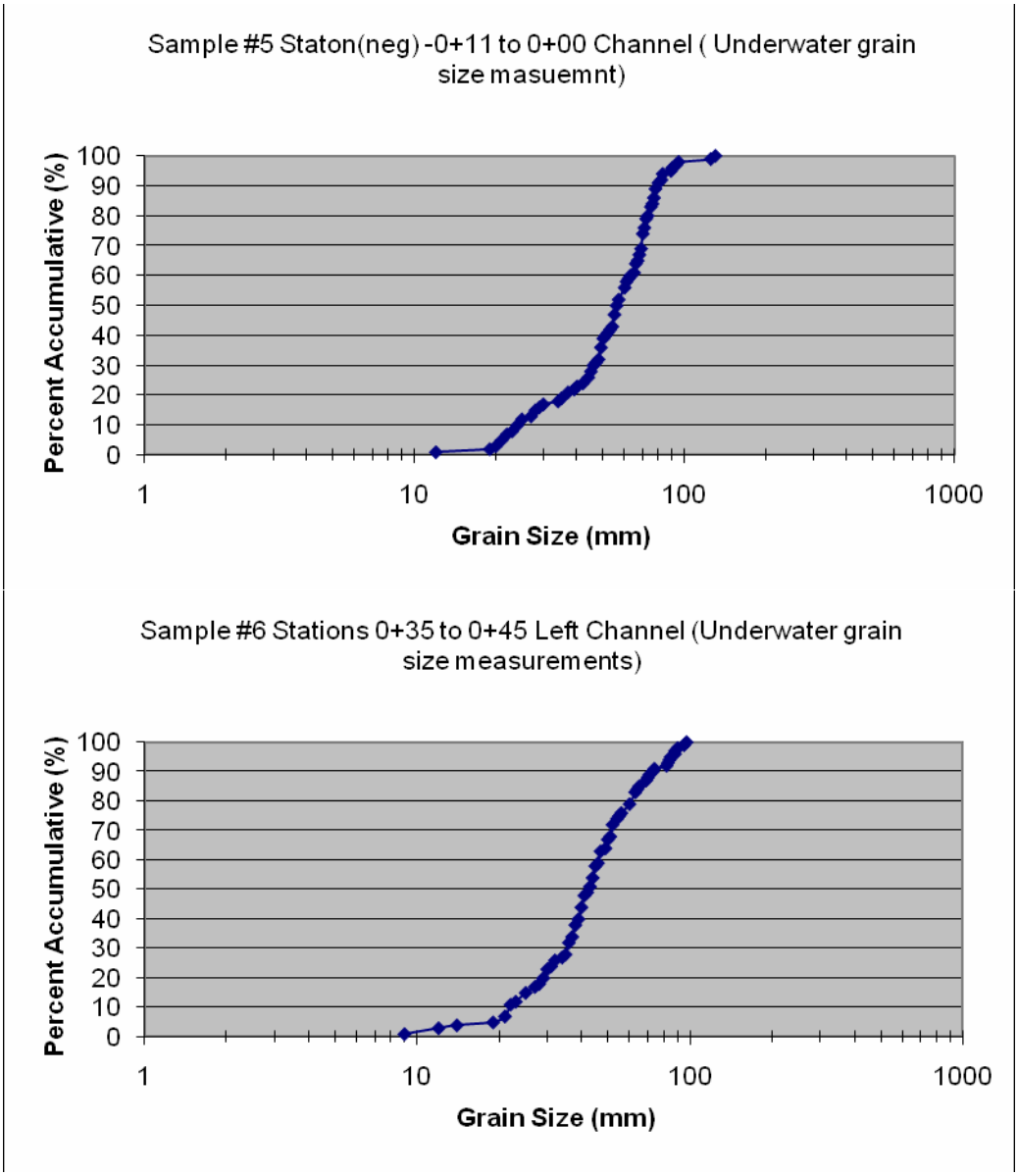
Sample #5 Staton(neg) -0+11 to 0+00 Channel (Underwater grain size masuemnt)
Percent Accumulative (%)
100
90
80
70
60
50
40
30
20
10
0
1
10
100
1000
Grain Size (mm)

Sample #6 Stations 0+35 to 0+45 Left Channel (Underwater grain size measurements)
Percent Accumulative (%)
100
90
80
70
60
50
40
30
20
10
0
1
10
100
1000
Grain Size (mm)

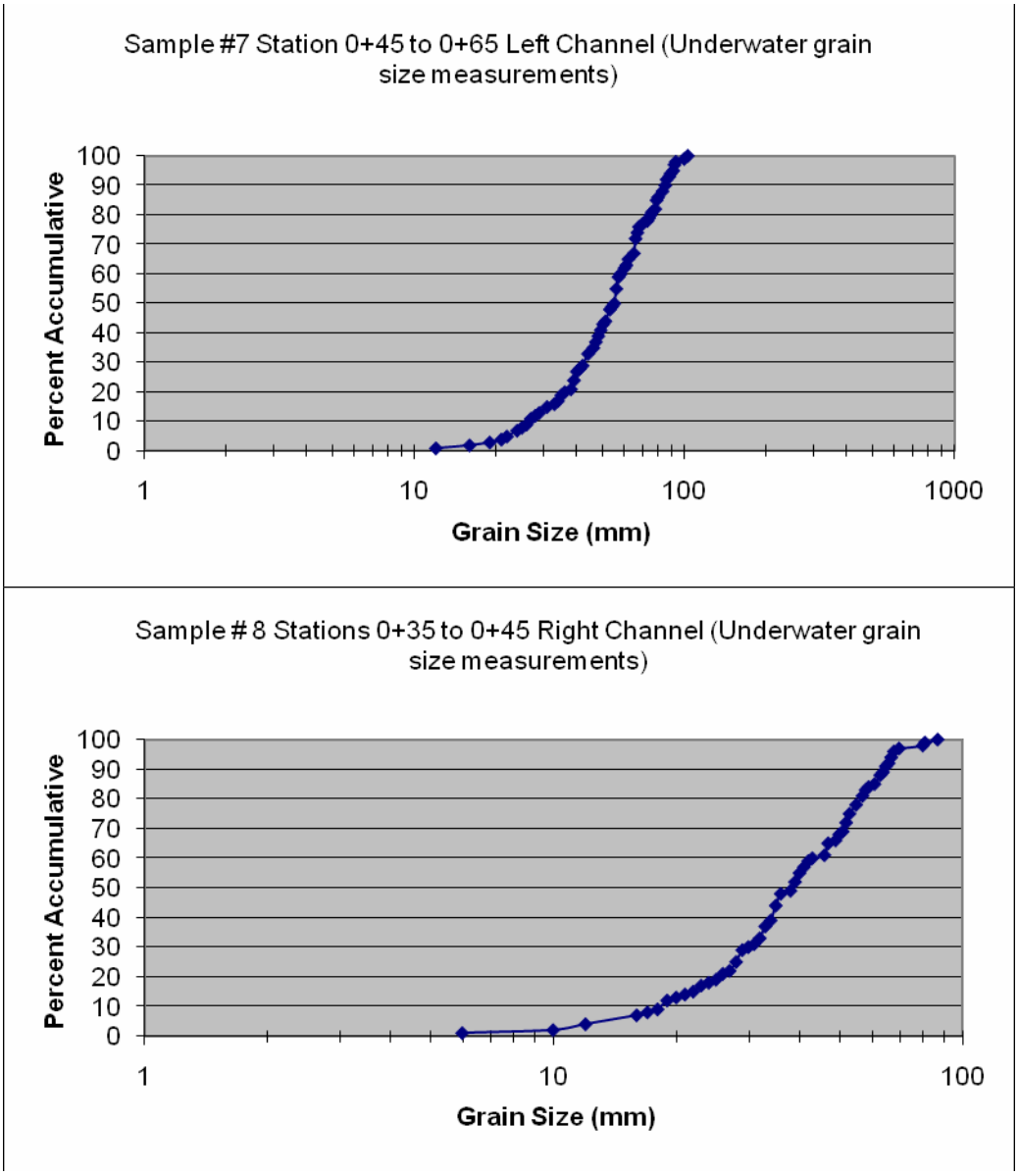
Sample #7 Station 0+45 to 0+65 Left Channel (Underwater grain size measurements)
Percent Accumulative
100
90
80
70
60
50
40
30
20
10
0
1
10
100
1000
Grain Size (mm)

Sample # 8 Stations 0+35 to 0+45 Right Channel (Underwater grain size measurements)
Percent Accumulative
100
90
80
70
60
50
40
30
20
10
0
1
10
100
Grain Size (mm)

Sample #9 Stations 0+45 to 0+65 Right Channel (Underwater grain size Measurements)

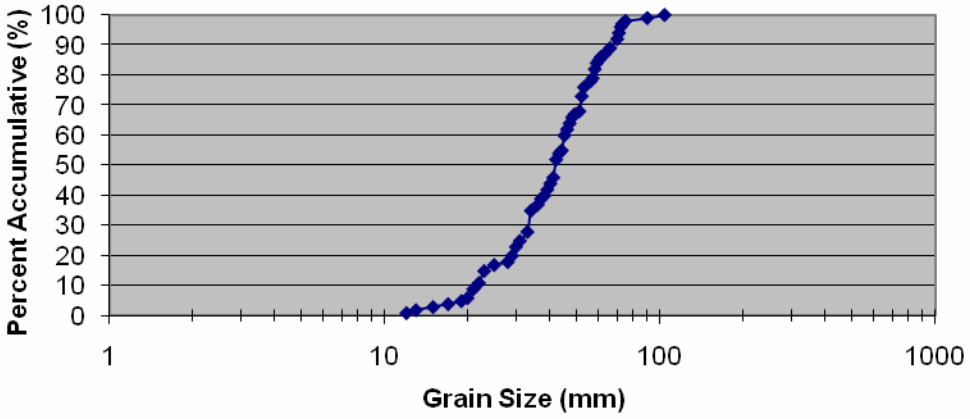

Sample #10 Stations 0+00 to 0+06 Channel (Underwater grain size measurements)

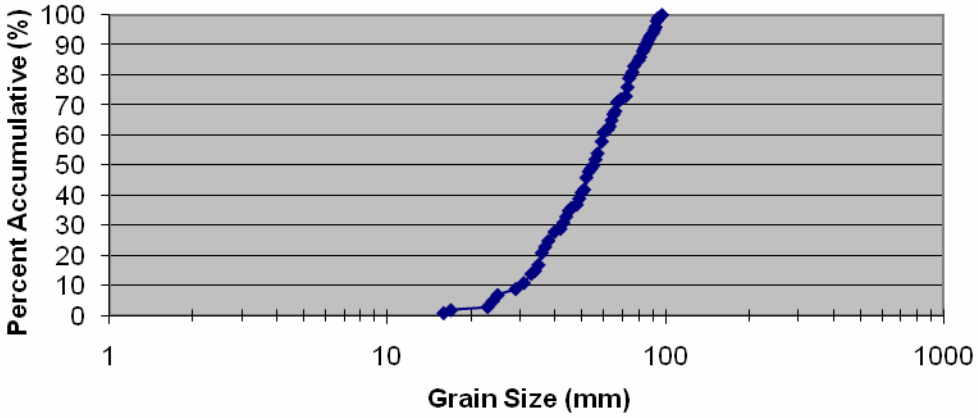

Appendix D: Gradient Graphs

Graident measurement graphs:

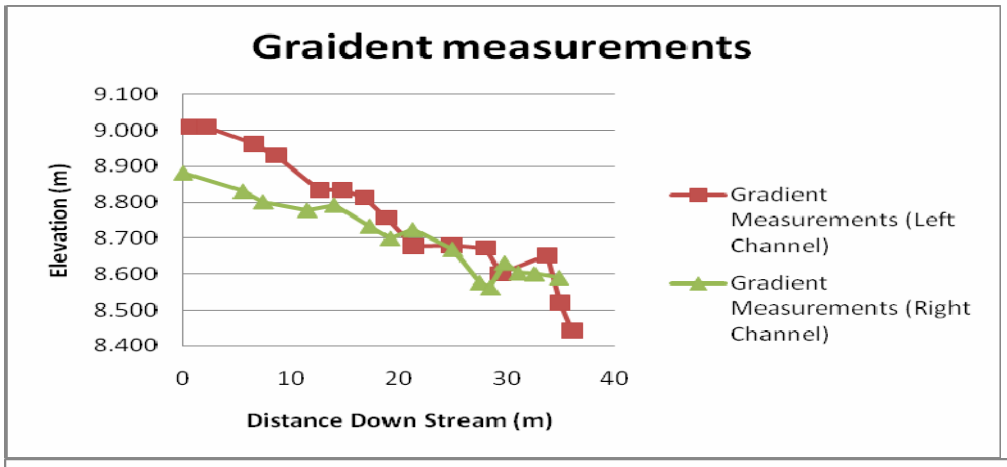

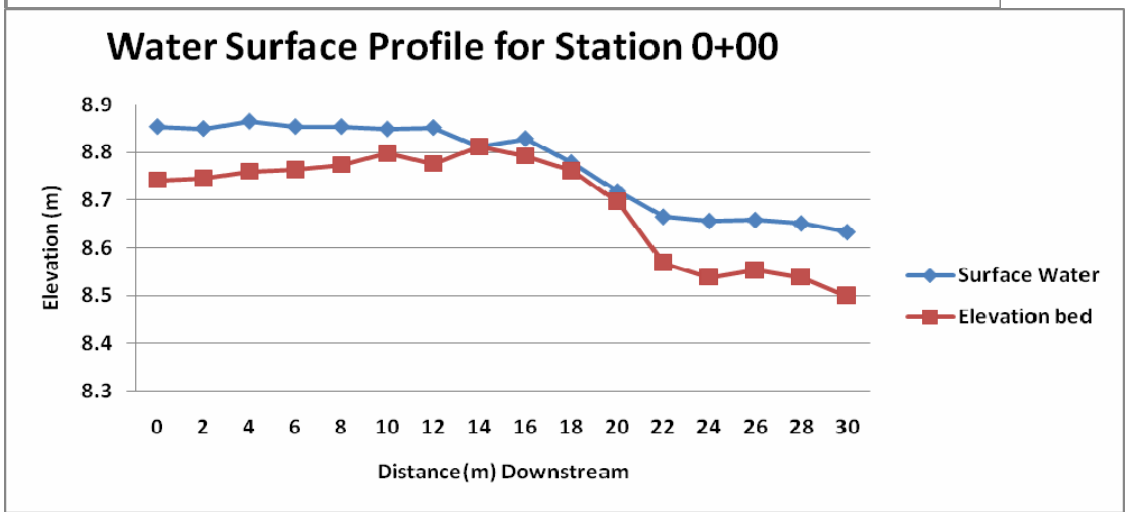

Appendix E: Dimensionless Shear Stress Data/calculations to create graphs. Cross-section 1,2,3,4,5,6,7, & 8

Dimensionless Shear Stress Graphs of cross sections (Red line represents Particle motion 0.045)

1)

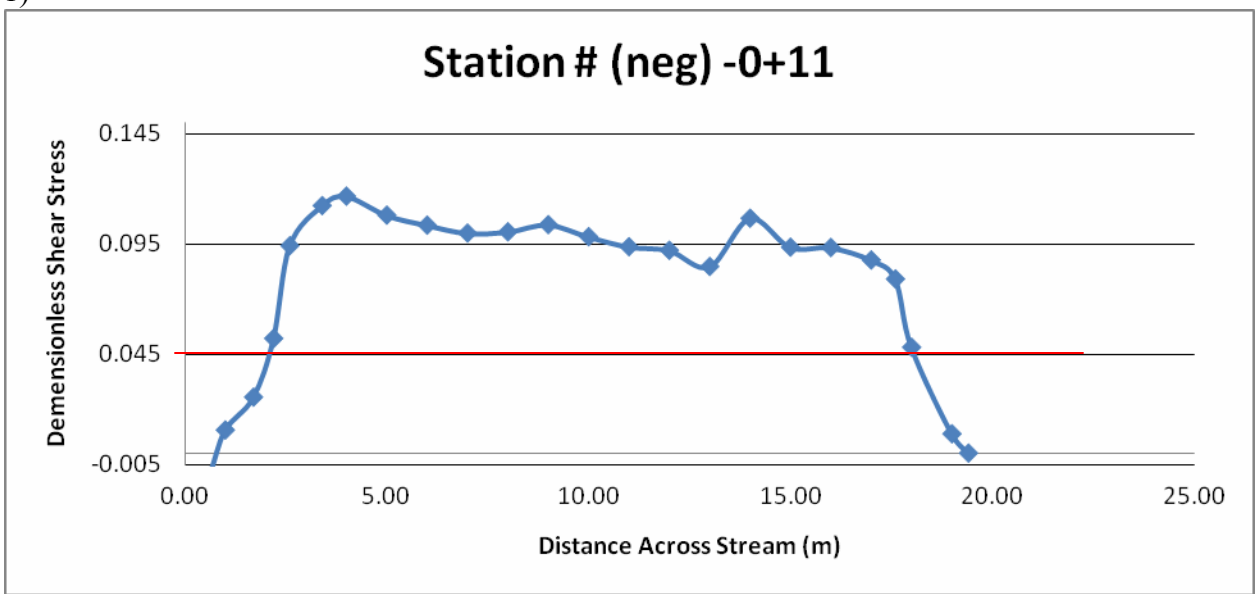

2)

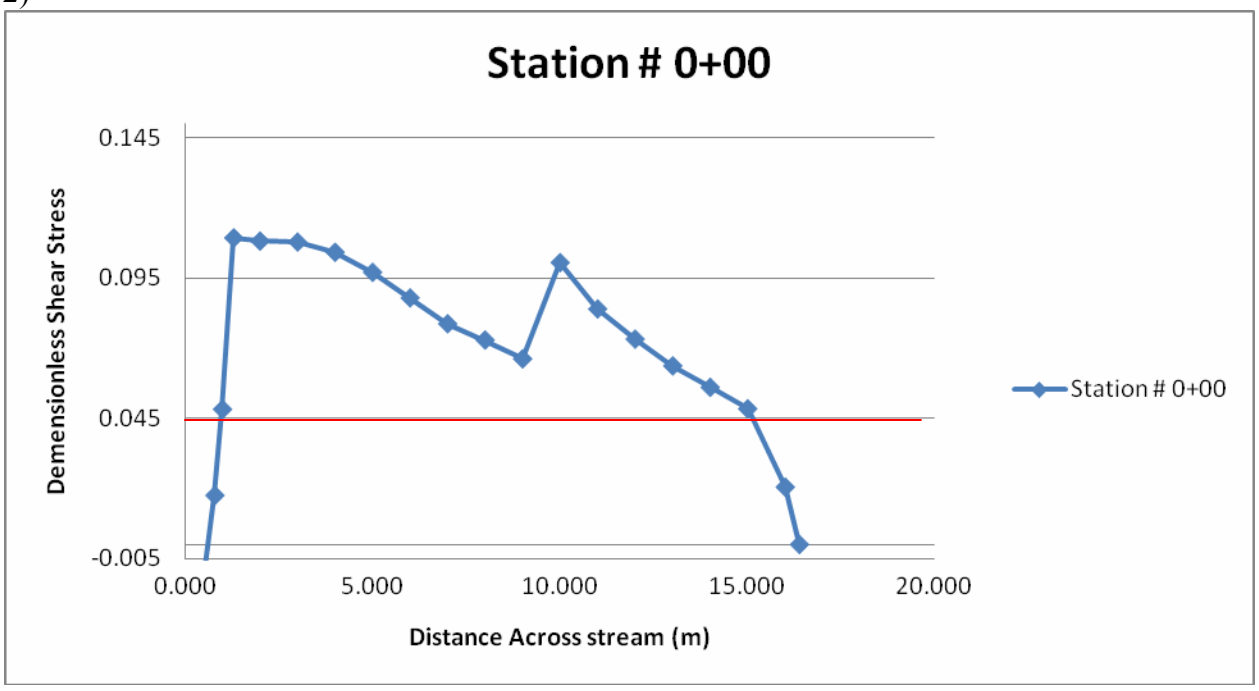

3)

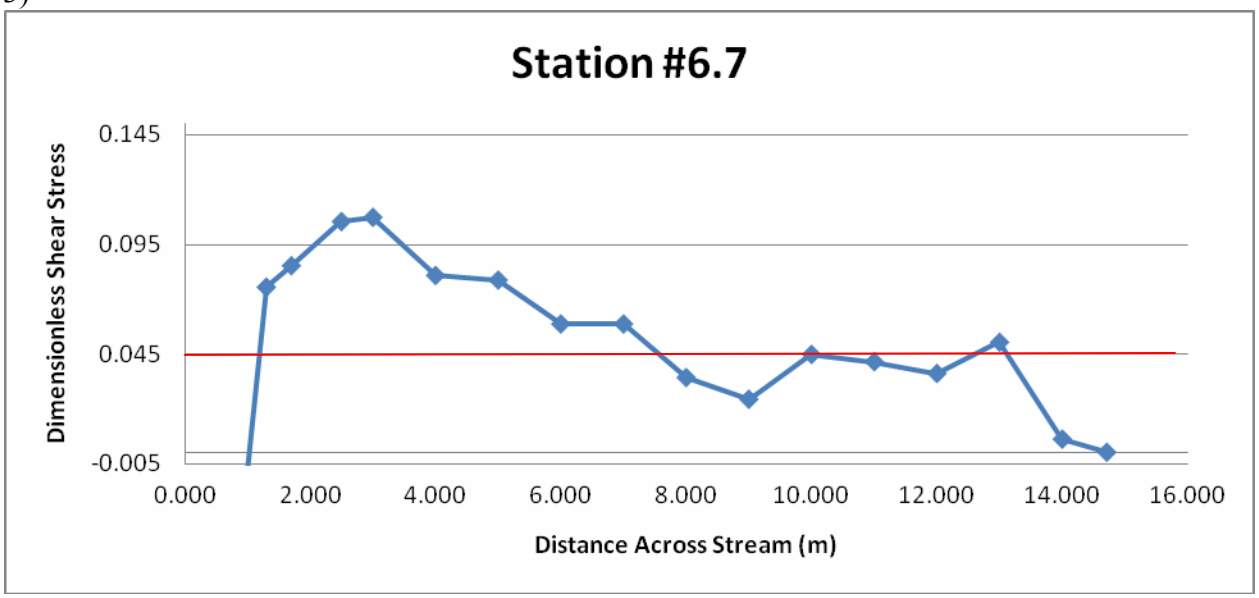
Station #6.7
Dimensionless Shear Stress
0.145
0.095
0.045
-0.005
0.000
2.000
4.000
6.000
8.000
10.000
12.000
14.000
16.000
Distance Across Stream (m)

4)

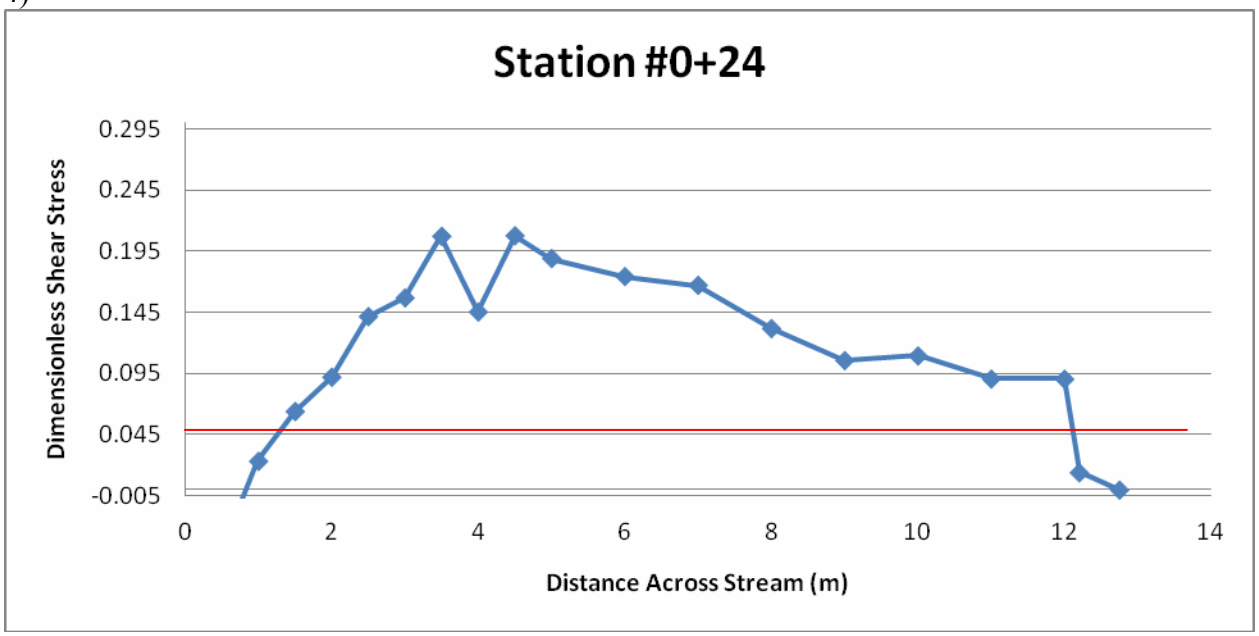
Station #0+24
Dimensionless Shear Stress
0.295
0.245
0.195
0.145
0.095
0.045
-0.005
0
2
4
6
8
10
12
14
Distance Across Stream (m)

5)

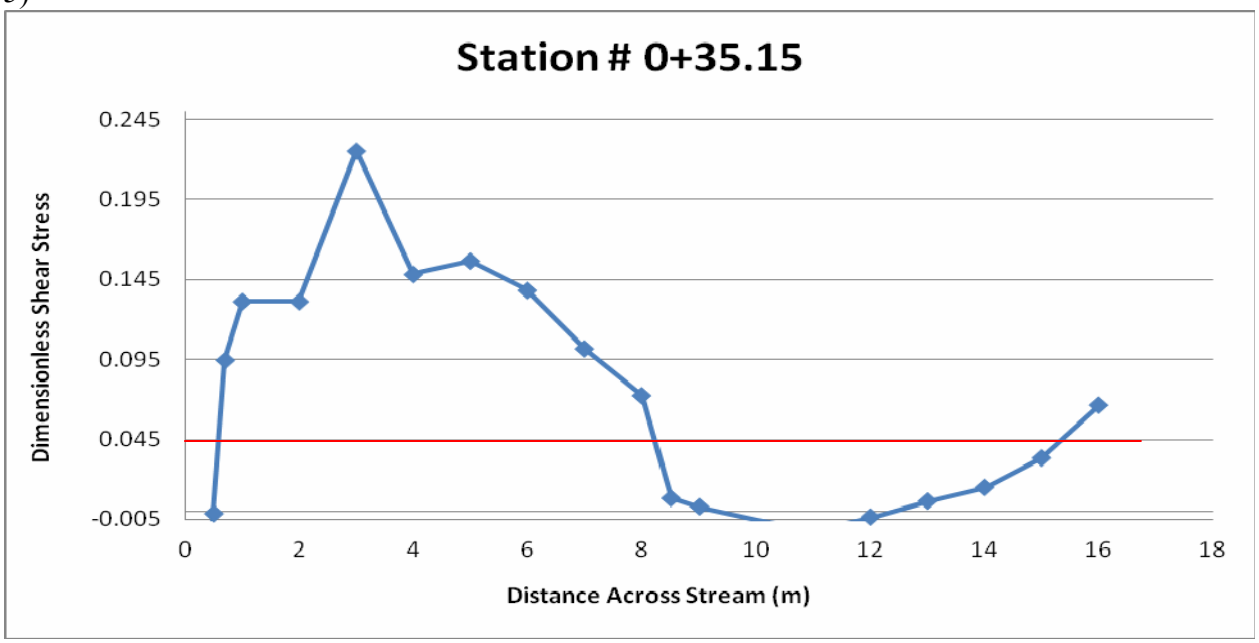
Station # 0+35.15
Dimensionless Shear Stress
0.245
0.195
0.145
0.095
0.045
-0.005
0
2
4
6
8
10
12
14
16
18
Distance Across Stream (m)

6)

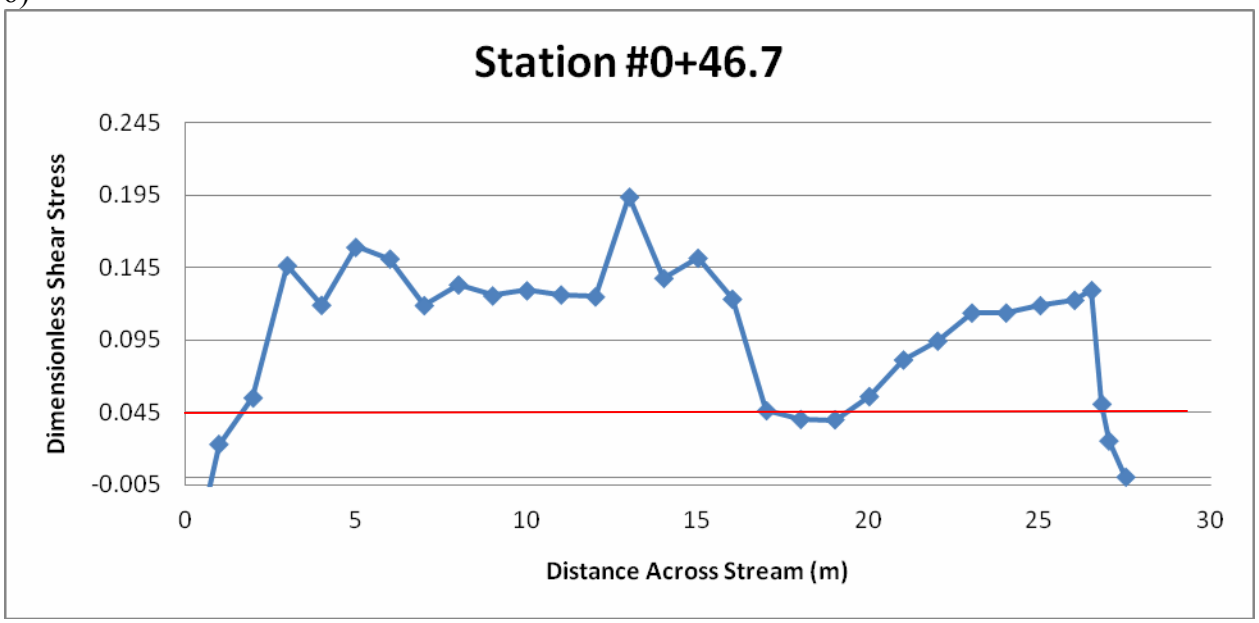
Station #0+46.7
Dimensionless Shear Stress
0.245
0.195
0.145
0.095
0.045
-0.005
0
5
10
15
20
25
30
Distance Across Stream (m)

7)

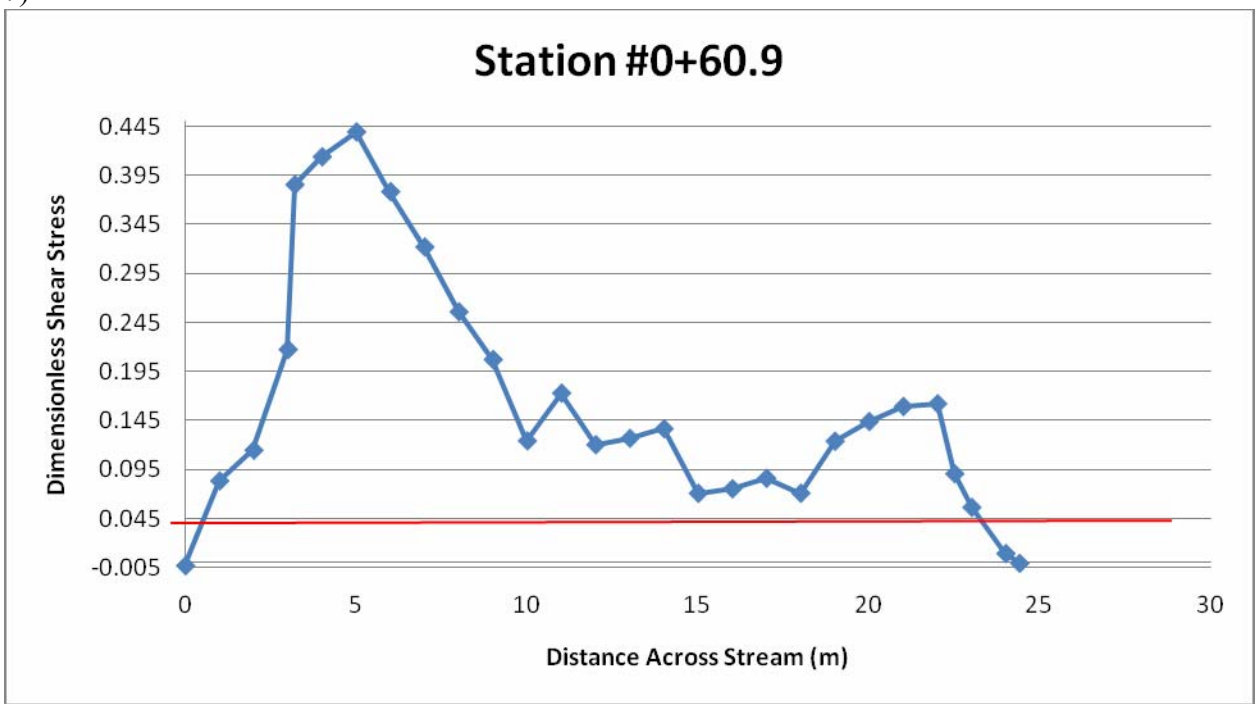
Station #0+60.9
Dimensionless Shear Stress
0.445
0.395
0.345
0.295
0.245
0.195
0.145
0.095
0.045
-0.005
0
5
10
15
20
25
30
Distance Across Stream (m)

8)

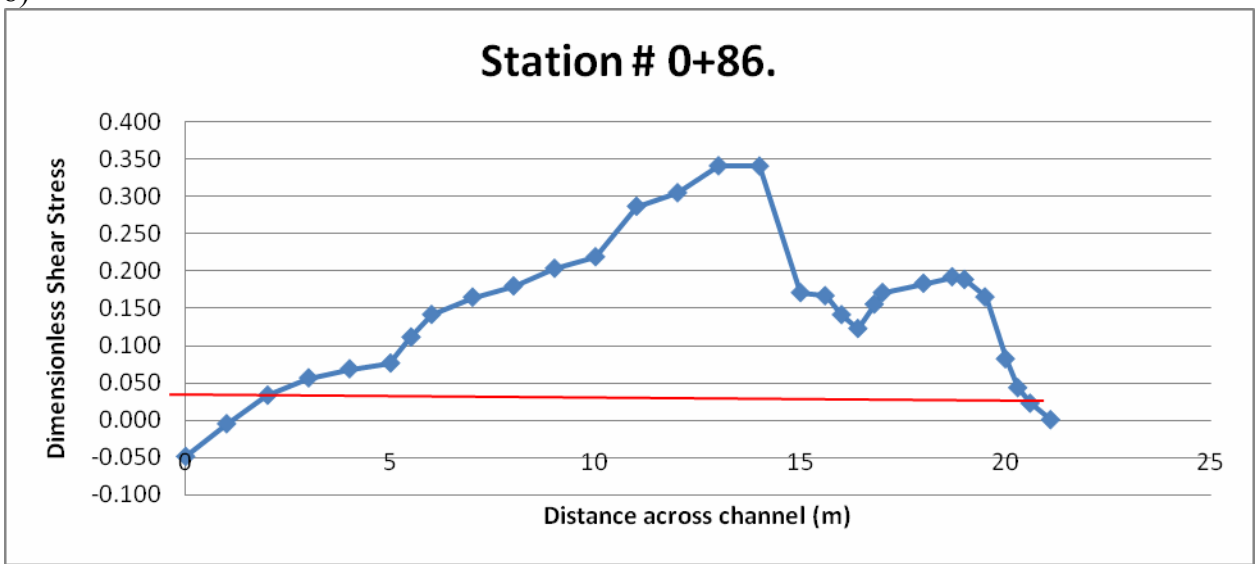
Station # 0+86.
Dimensionless Shear Stress
0.400
0.350
0.300
0.250
0.200
0.150
0.100
0.050
0.000
-0.050
-0.100
0
5
10
15
20
25
Distance across channel (m)